

ORIGINAL RESEARCH

Metabolic Signatures of Cardiac Dysfunction, Multimorbidity, and Post–Transcatheter Aortic Valve Implantation Death

Andrew S. Perry , MD; Shilin Zhao , PhD; Venkatesh Murthy , MD, PhD; Deepak K. Gupta , MD, MSCI; William F. Fearon , MD; Juyong B. Kim , MD; Samir Kapadia , MD; Dharam J. Kumbhani , MD; Linda Gillam , MD, MPH; Brian Whisenant , MD; Nishath Quader, MD; Alan Zajarias, MD; Ravinder R. Mallugari, MBBS; Daniel E. Clark , MD; Jay N. Patel , MD; Holly Gonzales, MD; Frederick G. Welt , MD; Anthony A. Bavry , MD; Megan Coylewright, MD, MPH; Robert N. Piana , MD; Anna Vatterott , MPH; Natalie Jackson , MPH; Robert E. Gerszten , MD; Brian R. Lindman , MD, MSCI*; Ravi Shah , MD*; Sammy Elmariah , MD, MPH*

BACKGROUND: Studies in mice and small patient subsets implicate metabolic dysfunction in cardiac remodeling in aortic stenosis, but no large comprehensive studies of human metabolism in aortic stenosis with long-term follow-up and characterization currently exist.

METHODS AND RESULTS: Within a multicenter prospective cohort study, we used principal components analysis to summarize 12 echocardiographic measures of left ventricular structure and function pre–transcatheter aortic valve implantation in 519 subjects (derivation). We used least absolute shrinkage and selection operator regression across 221 metabolites to define metabolic signatures for each structural pattern and measured their relation to death and multimorbidity in the original cohort and up to 2 validation cohorts (N=543 for overall validation). In the derivation cohort (519 individuals; median age, 84 years, 45% women, 95% White individuals), we identified 3 axes of left ventricular remodeling, broadly specifying systolic function, diastolic function, and chamber volumes. Metabolite signatures of each axis specified both known and novel pathways in hypertrophy and cardiac dysfunction. Over a median of 3.1 years (205 deaths), a metabolite score for diastolic function was independently associated with post–transcatheter aortic valve implantation death (adjusted hazard ratio per 1 SD increase in score, 1.54 [95% CI, 1.25–1.90]; $P<0.001$), with similar effects in each validation cohort. This metabolite score of diastolic function was simultaneously associated with measures of multimorbidity, suggesting a metabolic link between cardiac and noncardiac state in aortic stenosis.

CONCLUSIONS: Metabolite profiles of cardiac structure identify individuals at high risk for death following transcatheter aortic valve implantation and concurrent multimorbidity. These results call for efforts to address potentially reversible metabolic biology associated with risk to optimize post–transcatheter aortic valve implantation recovery, rehabilitation, and survival.

Key Words: aortic stenosis ■ metabolomics ■ outcomes ■ remodeling

Correspondence to: Sammy Elmariah, MD, MPH, Cardiology Division, Department of Medicine, University of California, San Francisco, 505 Parnassus Avenue, Room L523, Box 0103, San Francisco, CA 94143-0124. Email: sammy.elmariah@ucsf.edu

*B. R. Lindman, R. Shah, and S. Elmariah contributed equally.

This manuscript was sent to Sakima A. Smith, MD, MPH, Associate Editor, for review by expert referees, editorial decision, and final disposition.

Supplemental Material is available at <https://www.ahajournals.org/doi/suppl/10.1161/JAHA.123.029542>

For Sources of Funding and Disclosures, see page 11.

© 2023 The Authors. Published on behalf of the American Heart Association, Inc., by Wiley. This is an open access article under the terms of the [Creative Commons Attribution-NonCommercial-NoDerivs](https://creativecommons.org/licenses/by-nc-nd/4.0/) License, which permits use and distribution in any medium, provided the original work is properly cited, the use is non-commercial and no modifications or adaptations are made.

JAHA is available at: www.ahajournals.org/journal/jaha

CLINICAL PERSPECTIVE

What Is New?

- Metabolite signatures identified known and novel pathways of cardiac remodeling across a large sample of individuals with severe aortic stenosis referred for transcatheter aortic valve implantation.

What Are the Clinical Implications?

- A metabolic signature related to diastolic function was independently associated with post-transcatheter aortic valve implantation death and systemic multimorbidity (“frailty”) measures, suggesting links between cardiac and noncardiac states in advanced heart disease.

Nonstandard Abbreviations and Acronyms

AS	aortic stenosis
LASSO	least absolute shrinkage and selection operator
PC	principal component
PCA	principal components analysis
TAVI	transcatheter aortic valve implantation

While transcatheter aortic valve implantation (TAVI) improves outcome in individuals with symptomatic severe aortic stenosis (AS),¹ there remains significant residual risk following TAVI, marked by persistent poor quality of life and rehospitalization for heart failure (HF).^{2,3} As the application of TAVI in sicker populations with greater systemic comorbidity advances, identifying biological mechanisms of residual post-TAVI risk has become increasingly important, with risk assessment metrics based on clinical factors, cardiac-specific biomarkers, myocardial structure, and systemic illness.^{4–11} In this space, the growth of high-throughput methods for broad biochemical phenotyping (“omics”) has enabled a search for circulating biomarkers in a “hypothesis-free” discovery approach that may identify those individuals with reduced myocardial resilience, delineate underlying biological mechanisms, and identify opportunities for intervention to mitigate risk following TAVI. Our group and others have identified a series of metabolic pathways potentially linked to adverse remodeling in severe AS,^{12,13} several of which have been linked to systemic phenotypes previously relevant to post-TAVI risk (eg, “frailty”).¹⁴ Many of these “omic” studies are small, limited in phenotypic breadth, and lacking in significant follow-up to assess the relation between metabolism, adverse

phenotypes, and long-term outcome. Here, we address these central limitations by quantifying a broad circulating metabolome alongside detailed echocardiographic quantification of cardiac structure/function in individuals with symptomatic severe AS to delineate metabolic signatures and pathways related to cardiac remodeling and their relation to death and systemic multimorbidity. Our goal was to identify metabolic signatures of composite echocardiographic measures of cardiac remodeling characteristic in AS, using these metabolites to understand potential pathways and prognosis in AS.

METHODS

The data underlying this article will be shared upon reasonable request to the corresponding author.

Clinical Characterization

Our derivation cohort is a multicenter, prospective observational cohort study of adults with symptomatic severe AS undergoing TAVI between May 2014 and February 2017 (Data S1). Severe AS was defined according to American Society of Echocardiography guidelines: peak velocity ≥ 4 m/s, indexed aortic valve area $< 0.6 \text{ cm}^2/\text{m}^2$, or mean gradient $\geq 40 \text{ mmHg}$.¹⁵ We included participants in our derivation cohort whose pre-TAVI echocardiogram was transferred to our core laboratory for analysis with a pre-TAVI blood sample available. In addition to standard clinical and demographic indices, measures of systemic multimorbidity were obtained (eg, grip strength, gait speed, lung function, albumin, hemoglobin). Subjects in the derivation cohort underwent transthoracic echocardiography before TAVI (median, 39 days; interquartile range, 21–72). Echocardiograms were electronically transferred to our core laboratory to quantify left ventricular (LV) structure and function according to American Society of Echocardiography guidelines: LV ejection fraction (LVEF), LV stroke volume index, LV internal dimensions and volumes at end-diastole and end-systole, LV mass, relative wall thickness, mean transmitral E/e', tissue Doppler S velocity of lateral mitral annulus, left atrial volume, and mean aortic valve gradient.¹⁵

To test the relation of metabolic signatures of cardiac structure/function with death, we leveraged 2 additional cohorts: (1) a set of 286 individuals with blood samples from our parent multicenter, prospective observational cohort study who did not have full core lab-adjudicated echocardiographic phenotyping for analysis (therefore not included in derivation cohort); and (2) a single-center, prospective observational cohort study of 257 individuals with blood samples enrolled at Barnes-Jewish Hospital (St Louis, MO) with symptomatic severe AS who underwent TAVI between 2010 and 2015 (Figure S1). AS severity was defined according to American Society of Echocardiography criteria.

A complete assessment of vital status was performed between March and June 2020 for the multicenter cohort¹⁶ (both derivation and validation) and between November and December 2016 for the single-center cohort (validation).

Metabolite Profiling

Blood samples were obtained before TAVI in all participants. Metabolite profiling was performed via standard liquid chromatography–mass spectrometry techniques, details of which are summarized in Data S2.¹⁷

Analytic Methods

Generation of Composite Patterns of Cardiac Remodeling

Our analytic flow is shown in Figure 1. Our goal was to identify those metabolites related to cardiac structure/function in AS. Both “supervised” (phenotypic measures to “supervise” selection of metabolites related to that phenotype) and “unsupervised” methods (metabolome first reduced into sets of interrelated metabolites, agnostic to phenotype) have

been used recently in this regard to study phenotype-metabolome relation in HF.¹⁸ To build optimized models for composite measures of remodeling, we chose least absolute shrinkage and selection operator (LASSO) regression, in which >200 metabolites would be independent variables in models for a composite measure of cardiac structure/function (a supervised analytic approach). In contrast to some prior approaches focused on limited measures of cardiac remodeling (eg, LVEF, LV mass¹²), our experimental design incorporates measurement of multiple, related measures of remodeling by echocardiography to provide a more holistic assessment of cardiac structure/function. We used principal components analysis (PCA) to generate 3 composite axes of cardiac remodeling/function, resulting in participants having a principal component (PC) “score” for each axis (see Data S1 for further details).

LASSO Regression

To generate parsimonious models for each composite axis defined by PCA, we used LASSO regression (with

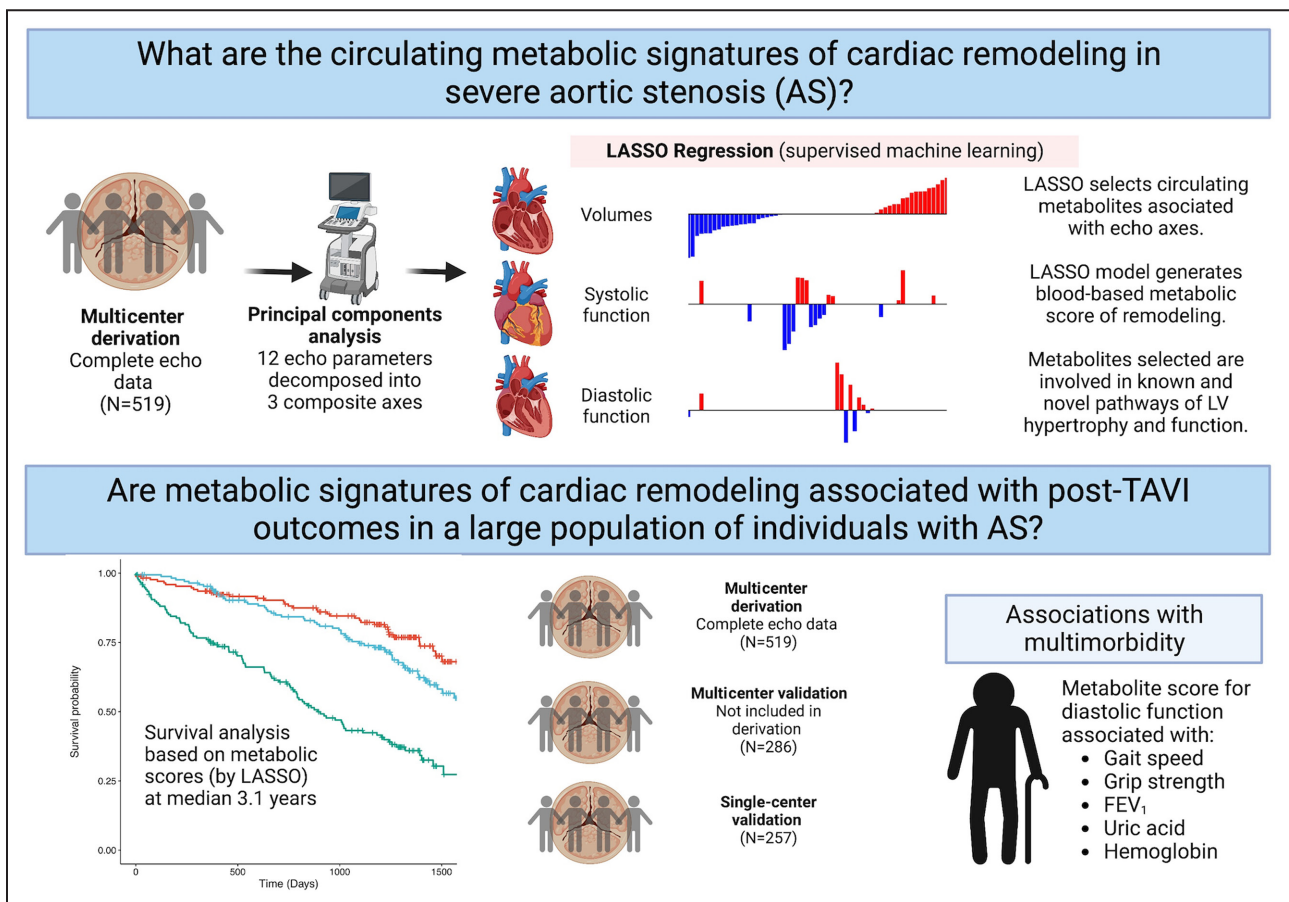


Figure 1. Overall study design.

FEV₁ indicates forced expiratory volume in the first second; LASSO, least absolute shrinkage and selection operator; LV, left ventricular; and TAVI, transcatheter aortic valve implantation. Created with BioRender.com.

10-fold cross validation to optimize hyper parameters; R package “glmnet”¹⁹ [R project; www.r-project.org]), with 3 PCA-based scores as the dependent variables and all metabolites as independent variables for selection. Metabolites were log-transformed to reduce skewness and standardized. LASSO models were used to generate “metabolite scores” (blood-based surrogates of the composite axes from PCA) in downstream analysis. To assess the pathway importance of each of the selected metabolites, we used pathway analysis (MetaboAnalyst 5.0; <https://www.metabolanalyst.ca>; accessed August 18, 2022) using the KEGG metabolome as reference²⁰ and literature search. The metabolites quantified in the single-center validation cohort did not completely match the metabolites measured in our multicenter cohort. Accordingly, we refit the LASSO models for use in the single-center cohort (see Data S1).

Survival Analysis

We standardized PC and metabolite scores for use in Cox models for all-cause death. Proportionality assumption for the metabolite scores were tested using the `cox.zph` function (R package “survival”) and examined Schoenfeld residuals for any suspected violation (by *P* value). For those with potential violations, models using robust standard errors were generated, yielding similar results to the original models. Hazard ratios (HRs) are reported per 1 SD difference in score, with standard 95% confidence intervals. Cox models were adjusted for age, sex, body mass index, diabetes (defined as hemoglobin A_{1c} ≥6.5% or reported history), coronary artery disease (defined as prior myocardial infarction, prior revascularization or atherosclerotic disease in ≥1 coronary arteries), history of atrial fibrillation/flutter, estimated glomerular filtration rate, cardiac troponin-T, and NT-proBNP (N-terminal pro-B-type natriuretic peptide). In the single-center validation cohort, we adjusted for the same variables except cardiac troponin-T or NT-proBNP due to unavailability) and B-type natriuretic peptide. To assess whether the metabolite-based scores would be independent of key echocardiographic phenotypes of risk following TAVI, we further adjusted for mean aortic valve gradient and LVEF in a sensitivity analysis. Biomarkers were log-transformed for use in Cox models.

Analyses were performed in R. All subjects provided informed consent as part of this research cohort. Institutional review boards at Vanderbilt University Medical Center and Massachusetts General Hospital approved this study.

RESULTS

Sample Characteristics

Characteristics of the 519 participants in our multicenter derivation cohort are reported in Table. The median

age was 84 years, with 45% women and 95% White individuals. The median Society of Thoracic Surgeons score was 4.2%. There was a high prevalence of both cardiovascular and noncardiovascular comorbidity, as well as abnormalities in cardiac structure (eg, LV hypertrophy), systolic (eg, LVEF), and diastolic function (elevated NT-proBNP, elevated E/e’). Characteristics of the validation cohorts were similar to our derivation cohort (Table).

Defining Composite Axes of Remodeling Using PCA of Echocardiographic Data

We observed significant interrelation across echocardiographic measures (Figure S2), motivating our approach to use PCA as an unsupervised method to summarize these related measures into composite “axes” of remodeling (see Analytic Methods). We identified 3 PCs that explained 65% of the variance in the data (Figure S3). Loadings for each of the 12 individual echocardiographic measures for each PC are shown in Figure 2A. The first PC was mostly weighted on LV volumes and LVEF (accordingly labeled “volumes”). The second PC was more highly loaded on stroke volume index and LVEF (accordingly labeled “systolic function”). The third PC was mostly loaded on E/e’ and left atrial volume (accordingly labeled “diastolic function”). When we visualized the 12 echocardiographic measures across our derivation cohort (Figure 2B), we observed (1) significant heterogeneity across individuals in cardiac structure/function (consistent with clinical practice) and (2) differences in PCA-based scores across individuals that appeared to track with this heterogeneity (color patterns on horizontal color bars, Figure 2B). These 3 PCA-based scores of composite axes of cardiac structure/function were carried forward to guide metabolic discovery.

Metabolic Signature of Cardiac Structure/Function in AS

We next aimed to define metabolomic correlates for cardiac structure/function, using the PCA-based composite axes in our derivation cohort. Sixty unique metabolites were selected in LASSO models (Table S1). Coefficients for metabolites from LASSO models (Figure S4) were used to generate metabolite-based scores for each PCA-based axis. We observed a moderate correlation of the metabolite scores with their parent PC scores (Figure S5; Spearman rho range, 0.41–0.47). We did not observe a clinically significant difference in metabolite scores by sex (Figure S6) and only a weak correlation with age (Figure 3; Tables S2 and S3). Individual metabolites across the 3 metabolite scores included metabolites previously implicated in cardiac structure and metabolism (long-chain

Table. Baseline Characteristics of the Multicenter Derivation, Multicenter Validation, and Single-Center Validation Cohorts

Characteristic	Derivation (N=519)	Multicenter validation (n=286)	Single-center validation (n=257)
Age, y	84 (78–88)	82 (75–87)	83 (76–89)
Sex, female	233 (45)	121 (42)	128 (50)
Race			
Black	17 (3.3)	1 (0.3)	
Asian	6 (1.2)	2 (0.7)	
White	495 (95)	282 (99)	251 (98)
Body mass index, kg/m ²	27.3 (23.8–31.4)	27.7 (24.6–32.9)	27.6 (23.9–31.3)
Diabetes	184 (36); 0.2	128 (45)	100 (39)
History of atrial fibrillation or flutter	200 (39); 0.4	122 (43); 0.3	104 (40)
Coronary artery disease	368 (71)	191 (67)	218 (85)
New York Heart Association class			
I	16 (3.3); 6.2	10 (3.7); 4.9	
II	140 (29); 6.2	47 (17); 4.9	
III	272 (56); 6.2	184 (68); 4.9	
IV	59 (12); 6.2	31 (11); 4.9	
Society of Thoracic Surgeons score	4.2 (2.9–6.3)	3.9 (2.6–6.3)	8.3 (5.0–12.6)
Echocardiographic measures before TAVI			
LV mass index, g/m ²	108 (91–126)	106 (91–127); 49	
LV hypertrophy by ASE criteria			
None	266 (51)	68 (47); 49	
Mild	87 (17)	33 (23); 49	
Moderate	69 (13)	20 (14); 49	
Severe	97 (19)	24 (17); 49	
LV ejection fraction (%)	61 (53–66)	60 (52–65); 9.1	60 (45–66); 0.4
LV ejection fraction <50%	106 (20)	55 (21); 9.1	79 (31); 0.4
Stroke volume index, mL/m ²	37 (30–45)	36 (28–43); 44	
Stroke volume index <35 mL/m ²	222 (43)	76 (48); 44	
LV end-diastolic internal diameter, mm	44 (40–49)	43 (39–49); 49	
LV end-systolic internal diameter, mm	29 (25–35)	29 (25–36); 50	
LV end-diastolic volume index, mL/m ²	44 (35–54)	45 (34–56); 58	
LV end-systolic volume index, mL/m ²	17 (12–25)	17 (12–29); 58	
Left atrial volume index, mL/m ²	35 (27–47)	39 (31–49); 48	
LV tissue Doppler S lateral annulus, cm/s	6.5 (5.3–7.8)	6.4 (5.4–7.3); 62	
Average transmitral E/e'	18 (14–24)	18 (14–24); 72	
Relative wall thickness	0.54 (0.45–0.64)	0.56 (0.49–0.65); 49	
Interventricular septum thickness, mm	12.6 (11.4–14.3)	13.2 (11.7–14.7); 49	
Posterior wall thickness, mm	11.8 (10.6–13.3)	12.5 (10.7–13.9); 49	
Aortic valve area, cm ²	0.72 (0.60–0.85); 0.2	0.73 (0.59–0.89); 12	0.70 (0.50–0.80); 1.2
Aortic valve area index, cm ² /m ²	0.39 (0.31–0.45); 0.2	0.37 (0.30–0.46); 12	
Aortic valve mean gradient, mmHg	39 (32–50)	38 (30–48); 8.0	41 (35–47); 0.4
Peak aortic velocity, m/s	4.09 (3.65–4.58); 0.2	4.01 (3.59–4.49); 13	
Moderate–severe aortic regurgitation	49 (9.4)	26 (9.1)	
Moderate–severe mitral regurgitation	72 (14)	36 (13)	
Laboratory measures before TAVI			
eGFR, mL/min per 1.73 m ²	54 (41–69); 0.4	54 (42–70); 1.0	55 (41–71)
NT-proBNP, ng/mL	1303 (622–3374); 3.5	1249 (560–2758); 2.1	

(Continued)

Table. Continued

Characteristic	Derivation (N=519)	Multicenter validation (n=286)	Single-center validation (n=257)
High-sensitivity cardiac troponin, ng/mL	25 (16–41); 3.5	24 (15–42); 2.1	
B-type natriuretic peptide, pg/mL			293 (154–658); 2.3

Continuous variables are reported as median (25th–75th percentile); % missing, if any. Categorical variables are reported as n (%); % missing. ASE indicates American Society of Echocardiography; eGFR, estimated glomerular filtration rate; LV, left ventricular; NT-proBNP, N-terminal pro-B-type natriuretic peptide; and TAVI, transcatheter aortic valve implantation.

acylcarnitines,¹² branched-chain amino acids²¹), as well as many not previously implicated in HF or AS (Table S1). Examining 52 metabolites with identifiable Human Metabolome Database identifiers across all 3 metabolite scores, we found several key enriched pathways (Figure S7): arginine metabolism (implicated in nitric oxide metabolism²²) and pantothenate and coenzyme A metabolism (central to aerobic metabolic flux²³), in addition to several others not widely previously implicated in cardiac remodeling.

Metabolite Scores of Cardiac Structure/Function in AS Are Associated With Death

We next measured the association of PC and metabolite scores with all-cause death in our derivation cohort (median follow-up, 3.1 years; 25th–75th percentile; 1.6–3.8 years; 205 deaths; Table S4). We did not observe meaningful violation of proportionality in Cox models (see Methods). While neither metabolite-based nor PC scores of LV volumes and systolic function were strongly and consistently related to outcome (Figure 4A), both the PC and metabolite-based scores of diastolic function were related to death. After adjustment for clinical risk factors and cardiac biomarkers, the metabolite score of diastolic function was associated with death (HR per 1 SD increase in score, 1.54 [95% CI, 1.25–1.90]; $P < 0.001$), which remained significant with further adjustments for mean aortic valve gradient and LVEF (HR per 1 SD increase, 1.55 [95% CI, 1.26–1.92]; $P < 0.001$). The PC score for diastolic function was directionally consistent (but not statistically significant). We observed similar results in the multicenter validation cohort (median follow-up, 2.6 years; 25th–75th percentile; 1.0–3.7 years; 121 deaths; Figure 4B). Using recalibrated metabolite scores in our single-center validation (recalibration fit [R^2] between 46% and 87%; Table S5; Figure S8), we observed an

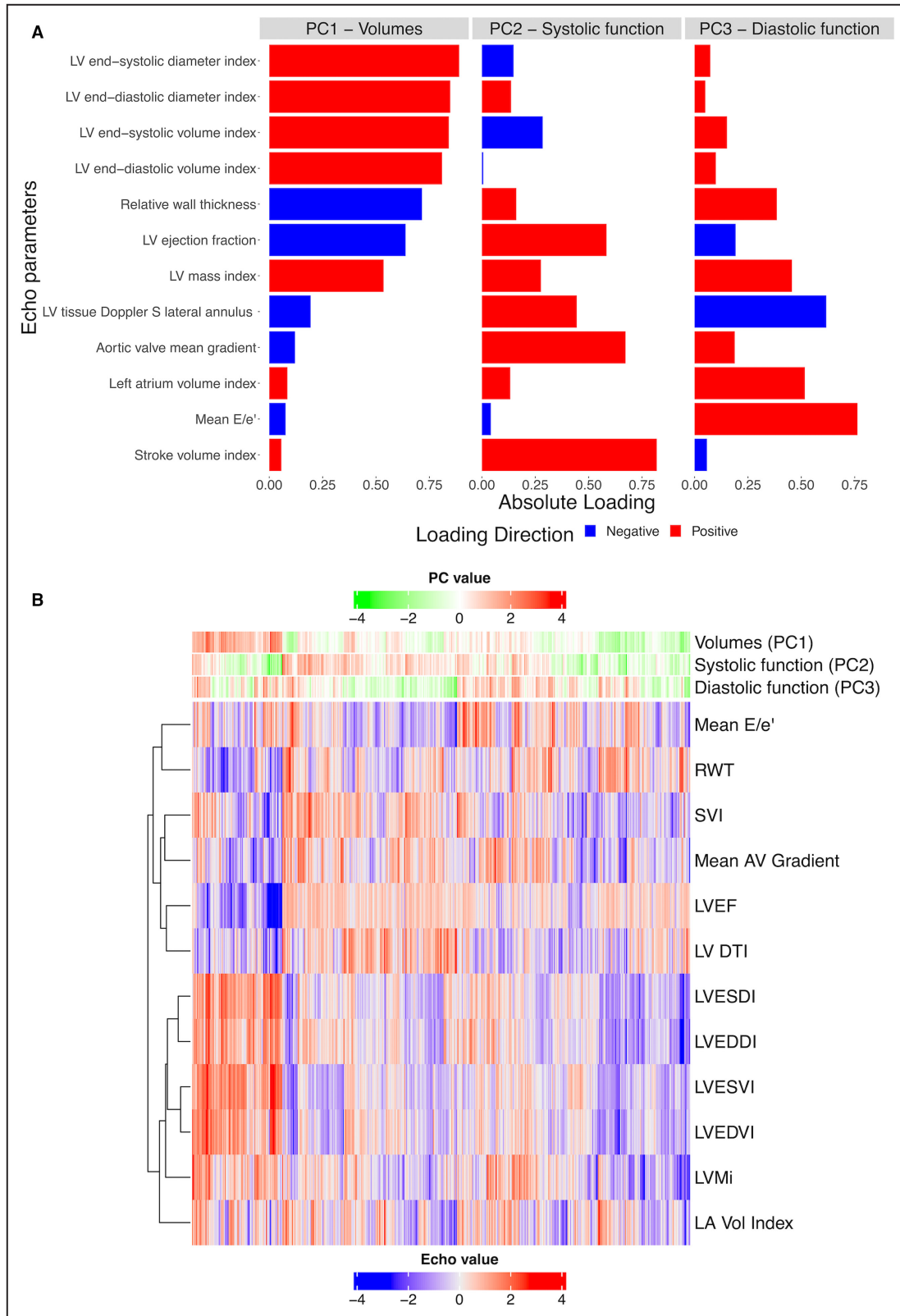
adjusted association between the metabolite score for PC3 (diastolic function)—but not PC1 or PC2—with death (median follow-up after TAVI, 1.6 years; 25th–75th percentile; 0.9–2.8 years; 93 events; Figure 4B and Figure S9).

Metabolites Associated With Cardiac Structure/Function Are Also Related to Functional Impairment Across Multiple Noncardiac Organ Systems

Despite the focus on cardiac structure/function to post-TAVI outcome,^{7,24} the importance of a holistic approach to assessing post-TAVI outcome (the concept of multimorbidity and frailty) is increasingly recognized as a major contributor to post-TAVI outcome not reversed completely by reduction in HF and restoration of cardiac performance.⁹ The finding that a metabolite score reflecting diastolic function (PC3)—a cardiac phenotype related in HF to other systems (eg, sarcopenia, obesity, inflammation¹⁸)—was associated with death across cohorts with adjustment for known post-TAVI risk was intriguing (Figure 4). We tested the hypothesis that metabolite-based scores may reflect noncardiac measures relevant to risk (distributions of multimorbidity measures are reported in Table S6). We observed a relation between the metabolite scores and multiorgan debility, particularly for the metabolite score corresponding to diastolic function (PC3; Figure 3, Tables S2 and S3). A higher metabolite score for diastolic function was related to higher uric acid (a marker of systemic inflammation²⁵), lower hemoglobin, and lower physical and pulmonary performance (Benjamini–Hochberg false discovery rate $< 5\%$ for all). Given that this metabolite score was not strongly related to age or sex (Figure 3, Figure S6), we excluded potential for confounding by age or sex, though other unmeasured confounders remain possible. Nevertheless, these analyses suggest

Figure 2. Interindividual heterogeneity in cardiac structure before TAVI.

A, Results of PCA of 12 echocardiographic measures. The bar plot indicates the PCA-based loadings for each echocardiographic measure for each PC. **B**, Clustered heatmap demonstrating individuals across echocardiographic measures, with PC scores for each individual represented as heatbars across the top of the heatmap. Each column is a participant, and rows represent phenotypes. AV indicates aortic valve; LA Vol, left atrium volume; LV DTI, tissue Doppler S velocity of lateral mitral annulus; LV, left ventricular; LVEDDI, left ventricular end-diastolic diameter index; LVEDVI, left ventricular end-diastolic volume index; LVEF, left ventricular ejection fraction; LVESDI, left ventricular end-systolic diameter index; LVESVI, left ventricular end-systolic volume index; LVMI, left ventricular mass index; PC, principal component; RWT, relative wall thickness; and SVI, stroke volume index.



that circulating metabolites of *cardiac* risk may also reflect additional *systemic multimorbidity*, potentially accounting for the prognostic performance of these metabolite patterns following TAVI.

DISCUSSION

While TAVI has revolutionized the care of individuals with severe AS, residual risk following TAVI remains

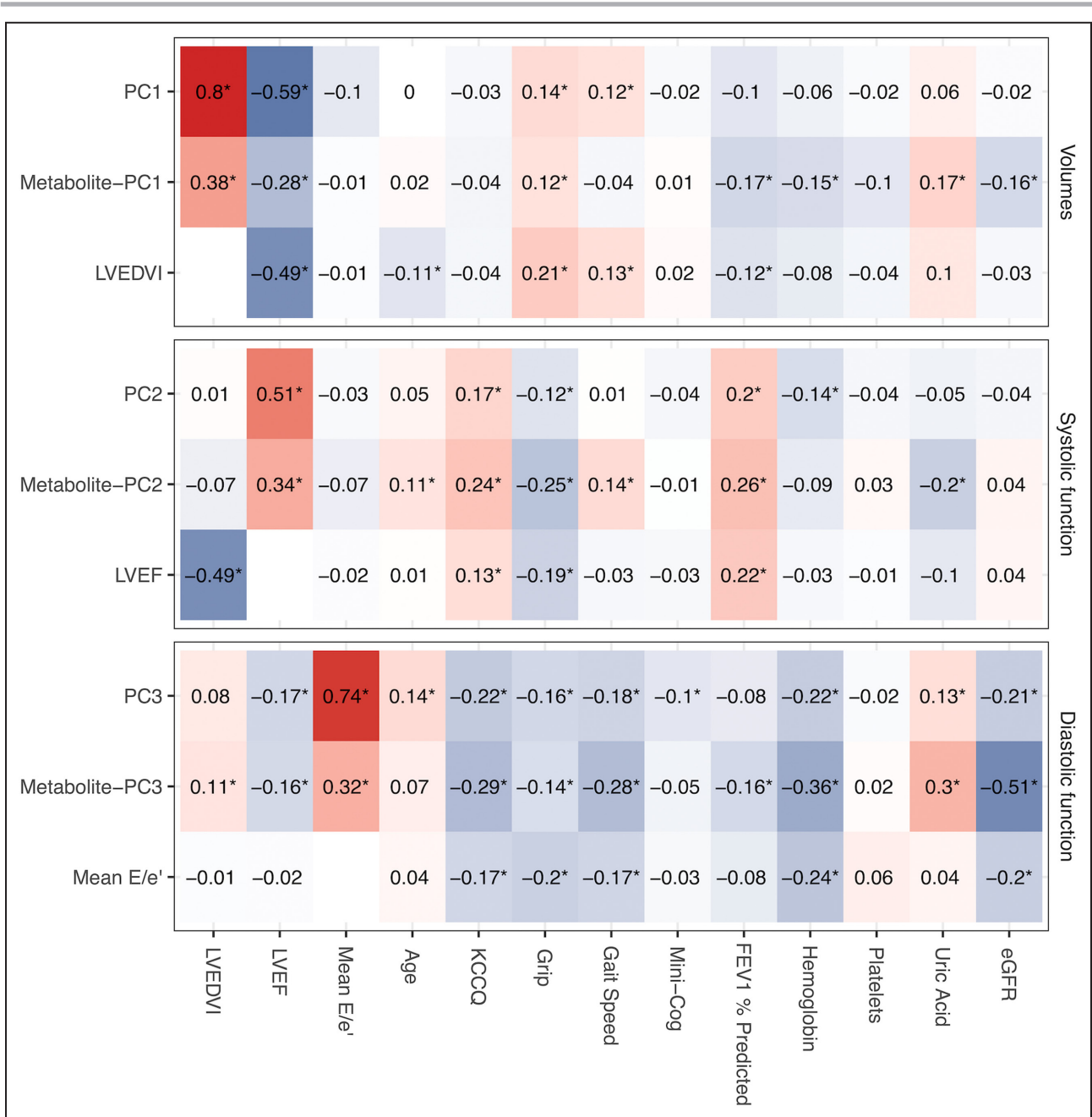


Figure 3. Metabolite scores are associated with measures of multimorbidity.

Spearman correlation between each metabolite PC scores and available measures of multimorbidity in the multicenter derivation cohort. Exemplary echocardiographic variables are also included (LVEDVI for volumes, PC1; LVEF for systolic function, PC2; Mean E/e' for diastolic function, PC3) to demonstrate the relation between each metabolite score with its exemplary LV phenotype. Raw data are reported in [Table S2](#). eGFR indicates estimated glomerular filtration rate; FEV₁, forced expiratory volume in the first second; KCCQ, Kansas City Cardiomyopathy Questionnaire summary score; LVEDVI, left ventricular end-diastolic volume index; LVEF, left ventricular ejection fraction; Mini-Cog, Mini-Cog score for dementia; and PC, principal component. *indicates a false discovery rate <0.05 (Benjamini-Hochberg method).

a significant clinical problem,^{2,3,6,26} reflecting multiple cardiac and noncardiac factors relevant to recovery and prognosis. While efforts in other advanced cardiac conditions (eg, HF) have been the subject of broad efforts to delineate mechanisms and biomarkers of risk, studies in AS are limited by study size and biomarker

and outcome characterization (beyond the short-term and standard clinical biomarkers). Here, we performed (to our knowledge) the largest study of individuals with symptomatic severe AS referred for TAVI before their procedure (1062 individuals), integrating comprehensive, core laboratory-adjudicated echocardiographic

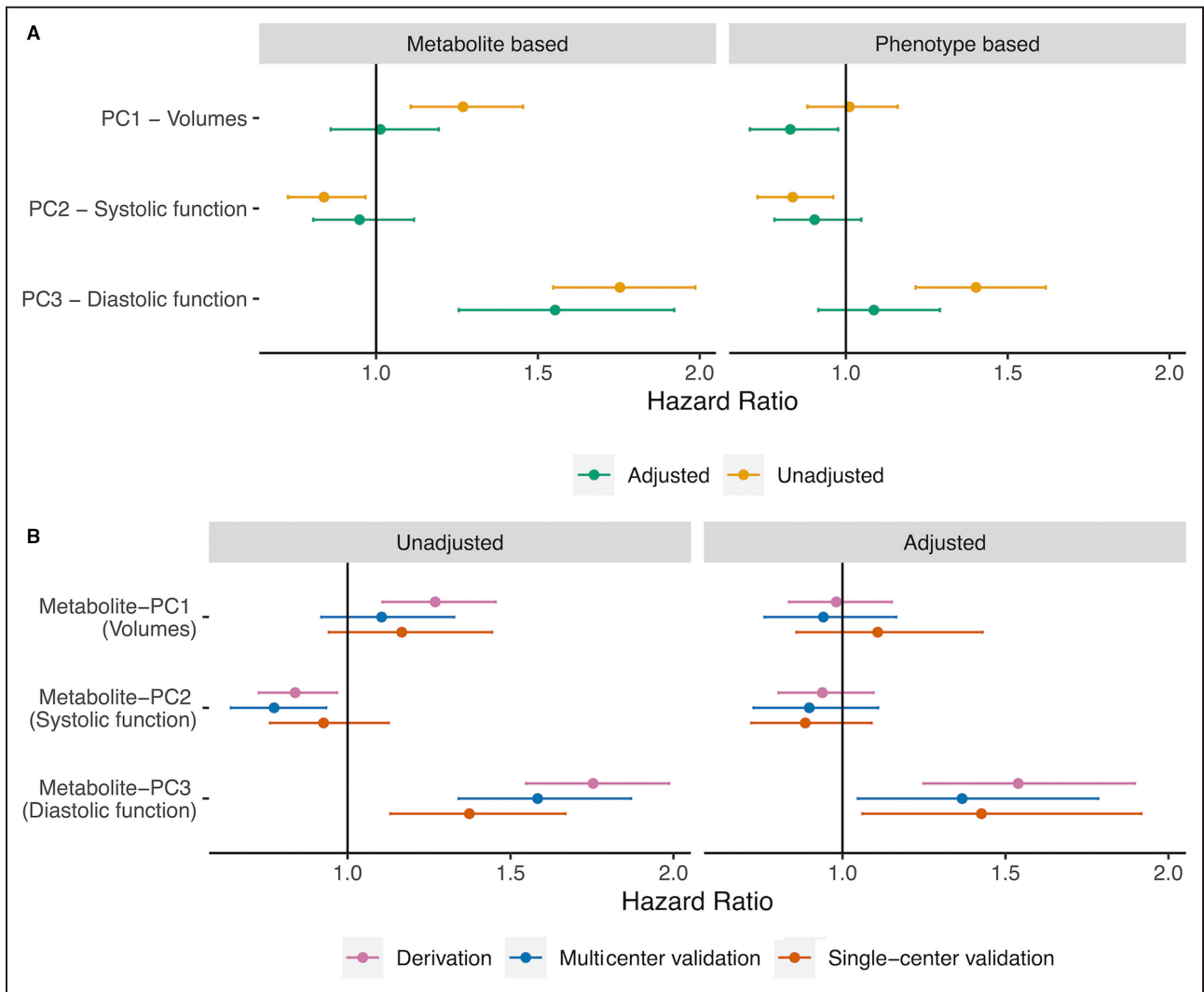


Figure 4. Association of metabolite scores and parent phenotype scores with death.

Results of Cox models are displayed with 95% CIs (model results in Table S5). **A**, Phenotype-based PC scores demonstrated limited associations with death after adjustment. The metabolite score for diastolic function (PC3) was associated with all-cause death. **B**, The association of each metabolite score with death in our replication cohorts, demonstrating replication of the prognostic association of our diastolic function metabolite score (PC3) with death in the multicenter and single-center validation cohorts. The effect sizes appear in a similar range as with the derivation cohort. PC indicates principal component.

measures with a broad metabolome to identify metabolic correlates of cardiac structure/function and their relation to death and morbidity. Our principal findings were 3-fold. First, using integrative statistical approaches, we defined metabolite signatures of 3 echocardiographic axes of remodeling (volumes, systolic and diastolic function), with the metabolite-based score corresponding to diastolic function related to long-term outcomes independent of known clinical risk factors, including markers of ischemia and hemodynamic stress. Second, metabolites reflecting each axis of cardiac remodeling identified both known and novel pathways related to remodeling. Third, a metabolite score that was constructed to reflect diastolic function was also related to systemic measures of organ-level

debility and dysfunction, including skeletal muscle, pulmonary, hematologic, and inflammatory systems. Collectively, in the largest cohort of individuals with metabolite profiling in AS, these findings underscore the relevance of systemic metabolism on both *cardiac* and *noncardiac* prognosis following TAVI.

Limited studies among patients with severe AS have demonstrated relationships between circulating metabolites (or their changes^{13,27}) and markers of adverse LV remodeling.^{12,13} Based on the importance of metabolism on cardiac function in previous work from our group¹² and others,^{28,29} we conducted one of the largest studies of metabolite profiling in severe AS, uniting detailed, core laboratory–adjudicated cardiac phenotyping with a broad metabolome to define

metabolic features associated with the pre-TAVI cardiac state. In our analysis, molecular signatures reflecting LV volumes and diastolic function (PC1 and PC3, respectively) included metabolites implicated in LV remodeling¹² (choline), hypertrophy³⁰ (uracil), survival among patients with HF³¹ (kynurenine), and coronary artery disease^{32,33} (S-adenosyl-L-homocysteine, C18:2 acylcarnitine). The metabolite signatures reflecting LV systolic function (PC2) included metabolites that appear protective against ischemia reperfusion injury³⁴ (N-oleoyl dopamine) and pressure overload-associated injury³⁵ (α -ketoglutaric acid). These results are consistent with prior work demonstrating a relationship between long-chain acylcarnitines and LV remodeling in 44 patients with severe AS¹² and a correlation between acylcarnitines and improvement of LVEF after TAVI in 30 patients.²⁷ Our results are consistent with other reports suggesting a role for nitric oxide metabolism in AS¹³ and incident HF.³⁶ A particularly interesting finding is the association of leucine and valine with diastolic function (PC3). Impaired metabolism of branched-chain amino acids has been implicated in the pathogenesis of HF, and pharmacological enhancement of this metabolic pathway may be of benefit.²¹ Importantly, several metabolites have not been widely reported in AS-related LV remodeling, suggesting potential for new discovery (Table S1).

In addition to metabolite relations, we found a striking relation between the metabolite score for PC3—the metabolic signature related to post-TAVI all-cause death—and measures of multiorgan function. These differences did not seem to be driven by differences in metabolite scores by sex (Figure S6) or age (Figure 3). One explanation may be due to a shared inflammatory pathophysiology of cardiac fibrosis/diastolic impairment and systemic organ function,³⁷ especially given the relation of persistent diastolic dysfunction²⁴ and underlying fibrosis^{38–40} on death following TAVI. An important corollary is the potential for reversibility in these cardiac phenotypes: Given the potential for rapid improvement in hemodynamics following TAVI, a shared metabolic signature between cardiac and noncardiac phenotypes may also identify individuals with lower metabolic “resiliency” to stress in noncardiac organs—“multimorbidity frailty.”⁴¹ Indeed, studies in humans and mice have identified shared factors relevant to cardiac hypertrophy responses to pressure overload and skeletal muscle metabolism,¹⁴ suggesting the potential for shared molecular pathways common to both cardiac and systemic “remodeling” following TAVI.

In effect, our findings provide molecular context for the emerging importance of cardiac-dependent and cardiac-independent frailty in advanced heart disease.⁴² While TAVI can immediately improve hemodynamics, it does not necessarily translate to improved frailty,⁴³ which is prognostically central.⁹ Certainly, we

do not advocate the use of these broad approaches to limit application of TAVI, given its dramatic impact on outcome.^{44–48} Nevertheless, approaches that quantify functional biomarkers of a systemic metabolic state (like this one) move the goalpost from identifying risk markers to limit TAVI toward efforts to understand potentially reversible biology associated with risk that represent opportunities for intervention. Whether additional interventions on this multimorbidity can reverse, or halt, some of these key biological processes remains an area of intense interest.

The results of this study should be viewed in the context of its design. While we explored concurrent phenotypes and metabolites (potential for reverse causation), the association of metabolite-based scores with long-term outcome increases confidence as to their validity. We did not evaluate for the confounding effects of medications. In addition, we did not examine changes in cardiac structure following TAVI. While evidence suggests that persistent fibrosis following TAVI may be central to future HF,⁴⁹ further studies in this cohort and others are required to understand how baseline pre-TAVI metabolism and changes following TAVI correspond to the capacity for reverse remodeling in the heart (and other organs). The cohorts studied underwent TAVI ≥ 5 years ago, which may limit generalizability to contemporary cohorts. Importantly, this study was performed in a predominantly White population, limiting generalizability to other racial and ethnic groups. Future studies with greater racial diversity that are based on the effects of intervention on a broad cardiac and noncardiac phenome will be helpful to delve further into the mechanistic and pathway relevance of selected metabolites.

In conclusion, we identified metabolite signatures of 3 distinct axes of cardiac structure/function, one of which was linked to long-term death after TAVI. Strikingly, a metabolic pattern of diastolic function was associated with multiorgan morbidity and frailty, highlighting an overlapping role of metabolism in cardiac and noncardiac states in advanced heart disease more generally. Studies to evaluate the effect of TAVI on metabolism—including adjunctive interventions to modify specific metabolic pathways—are needed to expand potential routes to optimize post-TAVI outcome.

ARTICLE INFORMATION

Received January 17, 2023; accepted May 25, 2023.

Affiliations

Vanderbilt Translational and Clinical Cardiovascular Research Center, Vanderbilt University School of Medicine, Nashville, TN (A.S.P., S.Z., D.K.G., R.R.M., H.G., R.N.P., A.V., N.J., B.R.L., R.S.); Department of Medicine and Radiology, University of Michigan, Ann Arbor, MI (V.M.); Department of Medicine, Division of Cardiology, Stanford Medical Center, Palo Alto, CA (W.F.F., J.B.K., D.E.C.); Department of Medicine, Division of Cardiology, Cleveland Clinic Foundation, Cleveland, OH (S.K.); Department of Medicine,

Division of Cardiology, University of Texas Southwestern Medical Center, Dallas, TX (D.J.K., A.A.B.); Department of Cardiovascular Medicine, Morristown Medical Center, Morristown, NJ (L.G.); Department of Medicine, Division of Cardiology, Intermountain Heart Institute, Murray, UT (B.W.); Department of Medicine, Division of Cardiology, Barnes-Jewish Hospital, St. Louis, MO (N.Q., A.Z.); Department of Medicine, Division of Cardiology, Ascension St. Thomas Hospital, Nashville, TN (J.N.P.); Department of Medicine, Division of Cardiology, University of Utah Hospital, Salt Lake City, UT (F.G.W.); Department of Internal Medicine, Division of Cardiovascular Medicine, Erlanger Heart and Lung Institute, Chattanooga, TN (M.C.); Cardiovascular Institute, Beth Israel Deaconess Medical Center, Harvard Medical School, Boston, MA (R.E.G.); Broad Institute of Harvard and MIT, Cambridge, MA (R.E.G.); and Department of Medicine, Division of Cardiology, The University of California, San Francisco, CA (S.E.).

Acknowledgments

The investigators thank the study participants for their contributions of time and biospecimens.

Sources of Funding

Metabolite quantification was funded by National Heart, Lung and Blood Institute, National Institutes of Health (R01-HL151838) (to Dr Elmariah). Echocardiographic phenotyping was funded by the Doris Duke Clinical Research Foundation (to Dr Lindman).

Disclosures

Dr Murthy has received grant support from Siemens Healthineers, National Institute of Diabetes and Digestive and Kidney Diseases, National Institute on Aging, National Heart, Lung, and Blood Institute, and the American Heart Association. He has received other research support from NIVA Medical Imaging Solutions. He owns stock in Eli Lilly, Johnson & Johnson, Merck, Bristol-Myers Squibb, and Pfizer and stock options in Ionetix. He has received research grants and speaking honoraria from Quart Medical. Dr Fearon receives institutional research support from Edwards, Abbott, Boston Scientific, and Medtronic. Dr Gillam is an advisor to Bracco Diagnostics, Philips, and Edwards Lifesciences and directs an imaging core laboratory with contracts with Edwards Lifesciences, Medtronic, and Abbott (no direct compensation). Dr Whisenant is a consultant at Edwards Lifescience and Medtronic. Dr Zajarias is a consultant at Edwards Lifescience. Dr Welt formerly sat on the Medtronic advisory board. Dr Coylewright received research funding from Edwards LifeSciences. Dr Piana serves on the data safety monitoring boards for Abbott Medical and Baim Cardiovascular Research Institute. Dr Gupta receives research support from Imara Inc. Dr Shah has received grant support from the National Institutes of Health and the American Heart Association and has served as a consultant in the past 12 months for Amgen and Cytokinetics. He is a coinventor on a patent for ex-RNA signatures of cardiac remodeling. Dr Lindman has served on the scientific advisory board for Roche Diagnostics and has received research grants from the National Institutes of Health (R01AG073633), Edwards Lifesciences, and Roche Diagnostics. Dr Elmariah has received research grants from Edwards Lifesciences, Medtronic, and Abbott and consulting fees from Edwards Lifesciences. The remaining authors have no disclosures to report.

Supplemental Material

Data S1
Tables S1–S6
Figures S1–S9
References 50–81

REFERENCES

- Leon MB, Smith CR, Mack M, Miller DC, Moses JW, Svensson LG, Tuzcu EM, Webb JG, Fontana GP, Makkar RR, et al. Transcatheter aortic-valve implantation for aortic stenosis in patients who cannot undergo surgery. *N Engl J Med*. 2010;363:1597–1607. doi: [10.1056/NEJMoa1008232](https://doi.org/10.1056/NEJMoa1008232)
- Arnold SV, Cohen DJ, Dai D, Jones PG, Li F, Thomas L, Baron SJ, Frankel NZ, Strong S, Matsouaka RA, et al. Predicting quality of life at 1 year after transcatheter aortic valve replacement in a real-world population. *Circ Cardiovasc Qual Outcomes*. 2018;11:e004693. doi: [10.1161/CIRCOUTCOMES.118.004693](https://doi.org/10.1161/CIRCOUTCOMES.118.004693)
- Vemulapalli S, Dai D, Hammill BG, Baron SJ, Cohen DJ, Mack MJ, Holmes DR Jr. Hospital resource utilization before and after transcatheter aortic valve replacement: the STS/ACC TVT registry. *J Am Coll Cardiol*. 2019;73:1135–1146. doi: [10.1016/j.jacc.2018.12.049](https://doi.org/10.1016/j.jacc.2018.12.049)
- Hermiller JB Jr, Yakubov SJ, Reardon MJ, Deeb GM, Adams DH, Afilalo J, Huang J, Popma JJ; CoreValve United States Clinical Investigators. Predicting early and late mortality after transcatheter aortic valve replacement. *J Am Coll Cardiol*. 2016;68:343–352. doi: [10.1016/j.jacc.2016.04.057](https://doi.org/10.1016/j.jacc.2016.04.057)
- Schoechlin S, Schulz U, Ruile P, Hein M, Eichenlaub M, Jander N, Neumann FJ, Valina C. Impact of high-sensitivity cardiac troponin T on survival and rehospitalization after transcatheter aortic valve replacement. *Catheter Cardiovasc Interv*. 2021;98:E881–E888. doi: [10.1002/ccd.29781](https://doi.org/10.1002/ccd.29781)
- Yoshijima N, Saito T, Inohara T, Anzai A, Tsuruta H, Shimizu H, Fukuda K, Naganuma T, Mizutani K, Yamawaki M, et al. Predictors and clinical outcomes of poor symptomatic improvement after transcatheter aortic valve replacement. *Open Heart*. 2021;8:e001742. doi: [10.1136/openhrt-2021-001742](https://doi.org/10.1136/openhrt-2021-001742)
- Gonzales H, Douglas PS, Pibarot P, Hahn RT, Khalique OK, Jaber WA, Cremer P, Weissman NJ, Asch FM, Zhang Y, et al. Left ventricular hypertrophy and clinical outcomes over 5 years after TAVR: an analysis of the PARTNER trials and registries. *JACC Cardiovasc Interv*. 2020;13:1329–1339. doi: [10.1016/j.jcin.2020.03.011](https://doi.org/10.1016/j.jcin.2020.03.011)
- Stein EJ, Fearon WF, Elmariah S, Kim JB, Kapadia S, Kumbhani DJ, Gillam L, Whisenant B, Quader N, Zajarias A, et al. Left ventricular hypertrophy and biomarkers of cardiac damage and stress in aortic stenosis. *J Am Heart Assoc*. 2022;11:e023466. doi: [10.1161/JAHA.121.023466](https://doi.org/10.1161/JAHA.121.023466)
- Afilalo J, Lauck S, Kim DH, Lefevre T, Piazza N, Lachapelle K, Martucci G, Lamy A, Labinaz M, Peterson MD, et al. Frailty in older adults undergoing aortic valve replacement: the FRAILTY-AVR study. *J Am Coll Cardiol*. 2017;70:689–700. doi: [10.1016/j.jacc.2017.06.024](https://doi.org/10.1016/j.jacc.2017.06.024)
- Kano S, Yamamoto M, Shimura T, Kagase A, Tsuzuki M, Kodama A, Koyama Y, Kobayashi T, Shibata K, Tada N, et al. Gait speed can predict advanced clinical outcomes in patients who undergo transcatheter aortic valve replacement: insights from a Japanese multicenter registry. *Circ Cardiovasc Interv*. 2017;10:e005088. doi: [10.1161/CIRCINTERVENTIONS.117.005088](https://doi.org/10.1161/CIRCINTERVENTIONS.117.005088)
- Edwards FH, Cohen DJ, O'Brien SM, Peterson ED, Mack MJ, Shahian DM, Grover FL, Tuzcu EM, Thourani VH, Carroll J, et al. Development and validation of a risk prediction model for in-hospital mortality after transcatheter aortic valve replacement. *JAMA Cardiol*. 2016;1:46–52. doi: [10.1001/jamacardio.2015.0326](https://doi.org/10.1001/jamacardio.2015.0326)
- Elmariah S, Farrell LA, Furman D, Lindman BR, Shi X, Morningstar JE, Rhee EP, Gerszten RE. Association of acylcarnitines with left ventricular remodeling in patients with severe aortic stenosis undergoing transcatheter aortic valve replacement. *JAMA Cardiol*. 2018;3:242–246. doi: [10.1001/jamacardio.2017.4873](https://doi.org/10.1001/jamacardio.2017.4873)
- van Driel BO, Schuldt M, Algul S, Levin E, Guclu A, Germans T, Rossum ACV, Pei J, Harakalova M, Baas A, et al. Metabolomics in severe aortic stenosis reveals intermediates of nitric oxide synthesis as most distinctive markers. *Int J Mol Sci*. 2021;22:3569. doi: [10.3390/ijms22073569](https://doi.org/10.3390/ijms22073569)
- Roh JD, Hobson R, Chaudhari V, Quintero P, Yeri A, Benson M, Xiao C, Zlotoff D, Bezzerides V, Houstis N, et al. Activin type II receptor signaling in cardiac aging and heart failure. *Sci Transl Med*. 2019;11:eaau8680. doi: [10.1126/scitranslmed.aau8680](https://doi.org/10.1126/scitranslmed.aau8680)
- Baumgartner H, Hung J, Bermejo J, Chambers JB, Edvardsen T, Goldstein S, Lancellotti P, LeFevre M, Miller F Jr, Otto CM. Recommendations on the echocardiographic assessment of aortic valve stenosis: a focused update from the European Association of Cardiovascular Imaging and the American Society of Echocardiography. *J Am Soc Echocardiogr*. 2017;30:372–392. doi: [10.1016/j.echo.2017.02.009](https://doi.org/10.1016/j.echo.2017.02.009)
- Perry AS, Stein EJ, Biersmith M, Fearon WF, Elmariah S, Kim JB, Clark DE, Patel JN, Gonzales H, Baker M, et al. Global longitudinal strain and biomarkers of cardiac damage and stress as predictors of outcomes after transcatheter aortic valve implantation. *J Am Heart Assoc*. 2022;11:e026529. doi: [10.1161/JAHA.122.026529](https://doi.org/10.1161/JAHA.122.026529)
- Zhou B, Xiao JF, Tuli L, Ransom HW. LC-MS-based metabolomics. *Mol Biosyst*. 2012;8:470–481. doi: [10.1039/c1mb05350g](https://doi.org/10.1039/c1mb05350g)
- Sanders-van Wijk S, Tromp J, Beussink-Nelson L, Hage C, Svedlund S, Saraste A, Swat SA, Sanchez C, Njoroge J, Tan RS, et al. Proteomic evaluation of the comorbidity-inflammation paradigm in heart failure with preserved ejection fraction: results from the PROMIS-HFpEF study. *Circulation*. 2020;142:2029–2044. doi: [10.1161/CIRCULATIONAHA.120.045810](https://doi.org/10.1161/CIRCULATIONAHA.120.045810)

19. Friedland JH, Hastie T, Tibshirani R. Regularization paths for generalized linear models via coordinate descent. *J Stat Softw*. 2010;33:1–22. doi: [10.18637/jss.v033.i01](https://doi.org/10.18637/jss.v033.i01)
20. Xia J, Psychogios N, Young N, Wishart DS. MetaboAnalyst: a web server for metabolomic data analysis and interpretation. *Nucleic Acids Res*. 2009;37:W652–W660. doi: [10.1093/nar/gkp356](https://doi.org/10.1093/nar/gkp356)
21. Sun H, Olson KC, Gao C, Prosdocimo DA, Zhou M, Wang Z, Jeyaraj D, Youn JY, Ren S, Liu Y, et al. Catabolic defect of branched-chain amino acids promotes heart failure. *Circulation*. 2016;133:2038–2049. doi: [10.1161/CIRCULATIONAHA.115.020226](https://doi.org/10.1161/CIRCULATIONAHA.115.020226)
22. Wu G, Morris SM Jr. Arginine metabolism: nitric oxide and beyond. *Biochem J*. 1998;336:1–17. doi: [10.1042/bj3360001](https://doi.org/10.1042/bj3360001)
23. Czumaj A, Szrok-Jurga S, Hebanowska A, Turyn J, Swierczynski J, Sledzinski T, Stelmanska E. The pathophysiological role of CoA. *Int J Mol Sci*. 2020;21:9057. doi: [10.3390/ijms21239057](https://doi.org/10.3390/ijms21239057)
24. Ong G, Pibarot P, Redfors B, Weissman NJ, Jaber WA, Makkar RR, Lerakis S, Gopal D, Khalique O, Kodali SK, et al. Diastolic function and clinical outcomes after transcatheter aortic valve replacement: PARTNER 2 SAPIEN 2 registry. *J Am Coll Cardiol*. 2020;76:2940–2951. doi: [10.1016/j.jacc.2020.10.032](https://doi.org/10.1016/j.jacc.2020.10.032)
25. Spiga R, Marini MA, Mancuso E, Di Fatta C, Fuoco A, Perticone F, Andreozzi F, Mannino GC, Sesti G. Uric acid is associated with inflammatory biomarkers and induces inflammation via activating the NF-kappaB signaling pathway in HepG2 cells. *Arterioscler Thromb Vasc Biol*. 2017;37:1241–1249. doi: [10.1161/ATVBAHA.117.309128](https://doi.org/10.1161/ATVBAHA.117.309128)
26. Tamburino C, Barbanti M, D'Errigo P, Ranucci M, Onorati F, Covello RD, Santini F, Rosato S, Santoro G, Fusco D, et al. 1-year outcomes after transfemoral transcatheter or surgical aortic valve replacement: results from the Italian OBSERVANT study. *J Am Coll Cardiol*. 2015;66:804–812. doi: [10.1016/j.jacc.2015.06.013](https://doi.org/10.1016/j.jacc.2015.06.013)
27. Haase D, Baz L, Bekfani T, Neugebauer S, Kiehnopf M, Mobius-Winkler S, Franz M, Schulze PC. Metabolomic profiling of patients with high gradient aortic stenosis undergoing transcatheter aortic valve replacement. *Clin Res Cardiol*. 2021;110:399–410. doi: [10.1007/s00392-020-01754-2](https://doi.org/10.1007/s00392-020-01754-2)
28. Cheng ML, Wang CH, Shiao MS, Liu MH, Huang YY, Huang CY, Mao CT, Lin JF, Ho HY, Yang NI. Metabolic disturbances identified in plasma are associated with outcomes in patients with heart failure: diagnostic and prognostic value of metabolomics. *J Am Coll Cardiol*. 2015;65:1509–1520. doi: [10.1016/j.jacc.2015.02.018](https://doi.org/10.1016/j.jacc.2015.02.018)
29. Hunter WG, Kelly JP, McGarrah RW III, Khouri MG, Craig D, Haynes C, Ilkayeva O, Stevens RD, Bain JR, Muehlbauer MJ, et al. Metabolomic profiling identifies novel circulating biomarkers of mitochondrial dysfunction differentially elevated in heart failure with preserved versus reduced ejection fraction: evidence for shared metabolic impairments in clinical heart failure. *J Am Heart Assoc*. 2016;5:5. doi: [10.1161/JAHA.115.003190](https://doi.org/10.1161/JAHA.115.003190)
30. Rossi A, Aussedat J, Olivares J, Ray A, Verdys M. Pyrimidine nucleotide metabolism in cardiac hypertrophy. *Eur Heart J*. 1984;5:155–162. doi: [10.1093/eurheartj/5.suppl_1.155](https://doi.org/10.1093/eurheartj/5.suppl_1.155)
31. Lund A, Nordrehaug JE, Slettom G, Solvang SH, Pedersen EK, Midttun O, Ulvik A, Ueland PM, Nygard O, Gilil LM. Plasma kynurenines and prognosis in patients with heart failure. *PLoS One*. 2020;15:e0227365. doi: [10.1371/journal.pone.0227365](https://doi.org/10.1371/journal.pone.0227365)
32. Zhang Z, Wang L, Zhan Y, Xie C, Xiang Y, Chen D, Wu Y. Clinical value and expression of Homer 1, homocysteine, S-adenosyl-L-homocysteine, fibroblast growth factors 23 in coronary heart disease. *BMC Cardiovasc Disord*. 2022;22:215. doi: [10.1186/s12872-022-02554-4](https://doi.org/10.1186/s12872-022-02554-4)
33. Deda O, Panteris E, Meikopoulos T, Begou O, Mouskeftara T, Karagiannidis E, Papazoglou AS, Sianos G, Theodoridis G, Gika H. Correlation of serum acylcarnitines with clinical presentation and severity of coronary artery disease. *Biomol Ther*. 2022;12:354. doi: [10.3390/biom12030354](https://doi.org/10.3390/biom12030354)
34. Zhong B, Wang DH. N-oleoyldopamine, a novel endogenous capsaicin-like lipid, protects the heart against ischemia-reperfusion injury via activation of TRPV1. *Am J Physiol Heart Circ Physiol*. 2008;295:H728–H735. doi: [10.1152/ajpheart.00022.2008](https://doi.org/10.1152/ajpheart.00022.2008)
35. An D, Zeng Q, Zhang P, Ma Z, Zhang H, Liu Z, Li J, Ren H, Xu D. Alpha-ketoglutarate ameliorates pressure overload-induced chronic cardiac dysfunction in mice. *Redox Biol*. 2021;46:102088. doi: [10.1016/j.redox.2021.102088](https://doi.org/10.1016/j.redox.2021.102088)
36. Tahir UA, Katz DH, Zhao T, Ngo D, Cruz DE, Robbins JM, Chen ZZ, Peterson B, Benson MD, Shi X, et al. Metabolomic profiles and heart failure risk in black adults: insights from the Jackson heart study. *Circ Heart Fail*. 2021;14:e007275. doi: [10.1161/CIRCHEARTFAILURE.120.007275](https://doi.org/10.1161/CIRCHEARTFAILURE.120.007275)
37. Paulus WJ, Zile MR. From systemic inflammation to myocardial fibrosis: the heart failure with preserved ejection fraction paradigm revisited. *Circ Res*. 2021;128:1451–1467. doi: [10.1161/CIRCRESAHA.121.318159](https://doi.org/10.1161/CIRCRESAHA.121.318159)
38. Thornton GD, Musa TA, Rigolli M, Loudon M, Chin C, Pica S, Malley T, Foley JRJ, Vassiliou VS, Davies RH, et al. Association of myocardial fibrosis and stroke volume by cardiovascular magnetic resonance in patients with severe aortic stenosis with outcome after valve replacement: the British Society of Cardiovascular Magnetic Resonance AS700 study. *JAMA Cardiol*. 2022;7:513–520. doi: [10.1001/jamacardio.2022.0340](https://doi.org/10.1001/jamacardio.2022.0340)
39. Everett RJ, Treibel TA, Fukui M, Lee H, Rigolli M, Singh A, Bijsterveld P, Tastet L, Musa TA, Dobson L, et al. Extracellular myocardial volume in patients with aortic stenosis. *J Am Coll Cardiol*. 2020;75:304–316. doi: [10.1016/j.jacc.2019.11.032](https://doi.org/10.1016/j.jacc.2019.11.032)
40. Papanastasiou CA, Kokkinidis DG, Kampaktis PN, Bikakis I, Cunha DK, Oikonomou EK, Greenwood JP, Garcia MJ, Karamitsos TD. The prognostic role of late gadolinium enhancement in aortic stenosis: a systematic review and meta-analysis. *JACC Cardiovasc Imaging*. 2020;13:385–392. doi: [10.1016/j.jcmg.2019.03.029](https://doi.org/10.1016/j.jcmg.2019.03.029)
41. Ijaz N, Buta B, Xue QL, Mohess DT, Bushan A, Tran H, Batchelor W, deFilippi CR, Walston JD, Bandeen-Roche K, et al. Interventions for frailty among older adults with cardiovascular disease: JACC state-of-the-art review. *J Am Coll Cardiol*. 2022;79:482–503. doi: [10.1016/j.jacc.2021.11.029](https://doi.org/10.1016/j.jacc.2021.11.029)
42. Flint KM, Matlock DD, Lindenfeld J, Allen LA. Frailty and the selection of patients for destination therapy left ventricular assist device. *Circ Heart Fail*. 2012;5:286–293. doi: [10.1161/CIRCHEARTFAILURE.111.963215](https://doi.org/10.1161/CIRCHEARTFAILURE.111.963215)
43. Gouda P, Paterson C, Meyer S, Shanks M, Butler C, Taylor D, Tyrrell B, Welsh R. Effects of transcatheter aortic valve implantation on frailty and quality of life. *CJC Open*. 2020;2:79–84. doi: [10.1016/j.cjco.2019.12.006](https://doi.org/10.1016/j.cjco.2019.12.006)
44. Bing R, Everett RJ, Tuck C, Semple S, Lewis S, Harkess R, Mills NL, Treibel TA, Prasad S, Greenwood JP, et al. Rationale and design of the randomized, controlled early valve replacement guided by biomarkers of left ventricular decompensation in asymptomatic patients with severe aortic stenosis (EVOLVED) trial. *Am Heart J*. 2019;212:91–100. doi: [10.1016/j.ahj.2019.02.018](https://doi.org/10.1016/j.ahj.2019.02.018)
45. Banovic M, Putnik S, Penicka M, Doros G, Deja MA, Kockova R, Kotrc M, Glaveckaite S, Gasparovic H, Pavlovic N, et al. Aortic valve replacement versus conservative treatment in asymptomatic severe aortic stenosis: the AVATAR trial. *Circulation*. 2022;145:648–658. doi: [10.1161/CIRCULATIONAHA.121.057639](https://doi.org/10.1161/CIRCULATIONAHA.121.057639)
46. Tastet L, Tribouilloy C, Marechaux S, Vollema EM, Delgado V, Salaun E, Shen M, Capoulade R, Clavel MA, Arsenault M, et al. Staging cardiac damage in patients with asymptomatic aortic valve stenosis. *J Am Coll Cardiol*. 2019;74:550–563. doi: [10.1016/j.jacc.2019.04.065](https://doi.org/10.1016/j.jacc.2019.04.065)
47. Lindman BR, Dweck MR, Lancellotti P, Genereux P, Pierard LA, O'Gara PT, Bonow RO. Management of asymptomatic severe aortic stenosis: evolving concepts in timing of valve replacement. *JACC Cardiovasc Imaging*. 2020;13:481–493. doi: [10.1016/j.jcmg.2019.01.036](https://doi.org/10.1016/j.jcmg.2019.01.036)
48. Lindman BR, Lindenfeld J. Prevention and mitigation of heart failure in the treatment of calcific aortic stenosis: a unifying therapeutic principle. *JAMA Cardiol*. 2021;6:993–994. doi: [10.1001/jamacardio.2021.2082](https://doi.org/10.1001/jamacardio.2021.2082)
49. Zhang C, Liu J, Qin S. Prognostic value of cardiac magnetic resonance in patients with aortic stenosis: a systematic review and meta-analysis. *PLoS One*. 2022;17:e0263378. doi: [10.1371/journal.pone.0263378](https://doi.org/10.1371/journal.pone.0263378)
50. Lewis GD, Wei R, Liu E, Yang E, Shi X, Martinovic M, Farrell L, Asnani A, Cyrille M, Ramanathan A, et al. Metabolite profiling of blood from individuals undergoing planned myocardial infarction reveals early markers of myocardial injury. *J Clin Invest*. 2008;118:3503–3512. doi: [10.1172/JCI35111](https://doi.org/10.1172/JCI35111)
51. Landoni G, Zangrillo A, Lomivorotov VV, Likhvantsev V, Ma J, De Simone F, Fominskiy E. Cardiac protection with phosphocreatine: a meta-analysis. *Interact Cardiovasc Thorac Surg*. 2016;23:637–646. doi: [10.1093/icvts/ivw171](https://doi.org/10.1093/icvts/ivw171)
52. Balestrino M. Role of creatine in the heart: health and disease. *Nutrients*. 2021;13:1215. doi: [10.3390/nu13041215](https://doi.org/10.3390/nu13041215)
53. Khlebnikov AI, Schepetkin IA, Quinn MT. Quantitative structure-activity relationships for small non-peptide antagonists of CXCR2: indirect 3D approach using the frontal polygon method. *Bioorg Med Chem*. 2006;14:352–365. doi: [10.1016/j.bmc.2005.08.026](https://doi.org/10.1016/j.bmc.2005.08.026)
54. Al Hageh C, Rahy R, Khazen G, Brial F, Khnayzer RS, Gauguier D, Zalloua PA. Plasma and urine metabolomic analyses in aortic valve stenosis reveal shared and biofluid-specific changes in metabolite levels. *PLoS One*. 2020;15:e0242019. doi: [10.1371/journal.pone.0242019](https://doi.org/10.1371/journal.pone.0242019)
55. Jou S, Patel H, Oglat H, Zhang R, Zhang L, Ellis P, Nappi A, El-Hajjar M, DeLago A, Torosoff M. The prevalence and prognostic implications

- of pre-procedural hyperbilirubinemia in patients undergoing transcatheter aortic valve replacement. *Heart Vessel*. 2020;35:1102–1108. doi: [10.1007/s00380-020-01588-y](https://doi.org/10.1007/s00380-020-01588-y)
56. Gall WE, Beebe K, Lawton KA, Adam KP, Mitchell MW, Nakhle PJ, Ryals JA, Milburn MV, Nannipieri M, Camastra S, et al. Alpha-hydroxybutyrate is an early biomarker of insulin resistance and glucose intolerance in a nondiabetic population. *PLoS One*. 2010;5:e10883. doi: [10.1371/journal.pone.0010883](https://doi.org/10.1371/journal.pone.0010883)
 57. Marszalek-Grabska M, Walczak K, Gawel K, Wicha-Komsta K, Wnorowska S, Wnorowski A, Turski WA. Kynurenine emerges from the shadows—current knowledge on its fate and function. *Pharmacol Ther*. 2021;225:107845. doi: [10.1016/j.pharmthera.2021.107845](https://doi.org/10.1016/j.pharmthera.2021.107845)
 58. Cluntun AA, Badolia R, Lettlova S, Parnell KM, Shankar TS, Diakos NA, Olson KA, Taleb I, Tatum SM, Berg JA, et al. The pyruvate-lactate axis modulates cardiac hypertrophy and heart failure. *Cell Metab*. 2021;33:629–648. doi: [10.1016/j.cmet.2020.12.003](https://doi.org/10.1016/j.cmet.2020.12.003)
 59. Guasch-Ferre M, Hu FB, Ruiz-Canela M, Bullo M, Toledo E, Wang DD, Corella D, Gomez-Gracia E, Fiol M, Estruch R, et al. Plasma metabolites from choline pathway and risk of cardiovascular disease in the PREDIMED (prevention with Mediterranean diet) Study. *J Am Heart Assoc*. 2017;6:e006524. doi: [10.1161/JAHA.117.006524](https://doi.org/10.1161/JAHA.117.006524)
 60. Stanford KI, Lynes MD, Takahashi H, Baer LA, Arts PJ, May FJ, Lehnig AC, Middelbeek RJW, Richard JJ, So K, et al. 12,13-diHOME: an exercise-induced lipokine that increases skeletal muscle fatty acid uptake. *Cell Metab*. 2018;27:1111–1120. doi: [10.1016/j.cmet.2018.03.020](https://doi.org/10.1016/j.cmet.2018.03.020)
 61. Raad M, AlBadri A, Wei J, Mehta PK, Maughan J, Gadh A, Thomson L, Jones DP, Quyyumi AA, Pepine CJ, et al. Oxidative stress is associated with diastolic dysfunction in women with ischemia with no obstructive coronary artery disease. *J Am Heart Assoc*. 2020;9:e015602. doi: [10.1161/JAHA.119.015602](https://doi.org/10.1161/JAHA.119.015602)
 62. Leary PJ, Tedford RJ, Bluemke DA, Bristow MR, Heckbert SR, Kawut SM, Krieger EV, Lima JA, Masri CS, Ralph DD, et al. Histamine H2 receptor antagonists, left ventricular morphology, and heart failure risk: the MESA study. *J Am Coll Cardiol*. 2016;67:1544–1552. doi: [10.1016/j.jacc.2016.01.045](https://doi.org/10.1016/j.jacc.2016.01.045)
 63. Chen J, Hong T, Ding S, Deng L, Abudupataer M, Zhang W, Tong M, Jia J, Gong H, Zou Y, et al. Aggravated myocardial infarction-induced cardiac remodeling and heart failure in histamine-deficient mice. *Sci Rep*. 2017;7:44007. doi: [10.1038/srep44007](https://doi.org/10.1038/srep44007)
 64. Mate-Munoz JL, Lougedo JH, Garnacho-Castano MV, Veiga-Herreros P, Lozano-Estevan MDC, Garcia-Fernandez P, de Jesus F, Guodemar-Perez J, San Juan AF, Dominguez R. Effects of beta-alanine supplementation during a 5-week strength training program: a randomized, controlled study. *J Int Soc Sports Nutr*. 2018;15:19. doi: [10.1186/s12970-018-0224-0](https://doi.org/10.1186/s12970-018-0224-0)
 65. Stefani GP, Capalonga L, da Silva LR, Dal Lago P. Beta-alanine and l-histidine supplementation associated with combined training increased functional capacity and maximum strength in heart failure rats. *Exp Physiol*. 2020;105:831–841. doi: [10.1113/EP088327](https://doi.org/10.1113/EP088327)
 66. Holm J, Ferrari G, Holmgren A, Vanky F, Friberg O, Vidlund M, Svedjeholm R. Effect of glutamate infusion on NT-proBNP after coronary artery bypass grafting in high-risk patients (GLUTAMICS II): a randomized controlled trial. *PLoS Med*. 2022;19:e1003997. doi: [10.1371/journal.pmed.1003997](https://doi.org/10.1371/journal.pmed.1003997)
 67. Sivakumar R, Babu PV, Shyamaladevi CS. Aspartate and glutamate prevents isoproterenol-induced cardiac toxicity by alleviating oxidative stress in rats. *Exp Toxicol Pathol*. 2011;63:137–142. doi: [10.1016/j.etp.2009.10.008](https://doi.org/10.1016/j.etp.2009.10.008)
 68. Zheng Y, Hu FB, Ruiz-Canela M, Clish CB, Dennis C, Salas-Salvado J, Hruby A, Liang L, Toledo E, Corella D, et al. Metabolites of glutamate metabolism are associated with incident cardiovascular events in the PREDIMED PREvención con Dieta Mediterránea (PREDIMED) trial. *J Am Heart Assoc*. 2016;5:e003755. doi: [10.1161/JAHA.116.003755](https://doi.org/10.1161/JAHA.116.003755)
 69. Krylova IB, Selina EN, Bulion VV, Rodionova OM, Evdokimova NR, Belosludtseva NV, Shigaeva MI, Mironova GD. Uridine treatment prevents myocardial injury in rat models of acute ischemia and ischemia/reperfusion by activating the mitochondrial ATP-dependent potassium channel. *Sci Rep*. 2021;11:16999. doi: [10.1038/s41598-021-96562-7](https://doi.org/10.1038/s41598-021-96562-7)
 70. Salmani M, Alipoor E, Navid H, Farahbakhsh P, Yaseri M, Imani H. Effect of l-arginine on cardiac reverse remodeling and quality of life in patients with heart failure. *Clin Nutr*. 2021;40:3037–3044. doi: [10.1016/j.clnu.2021.01.044](https://doi.org/10.1016/j.clnu.2021.01.044)
 71. Deidda M, Piras C, Dessalvi CC, Locci E, Barberini L, Torri F, Ascedu F, Atzori L, Mercurio G. Metabolomic approach to profile functional and metabolic changes in heart failure. *J Transl Med*. 2015;13:297. doi: [10.1186/s12967-015-0661-3](https://doi.org/10.1186/s12967-015-0661-3)
 72. Shimada YJ, Batra J, Kochav SM, Patel P, Jung J, Maurer MS, Hasegawa K, Reilly MP, Fifer MA. Difference in metabolomic response to exercise between patients with and without hypertrophic cardiomyopathy. *J Cardiovasc Transl Res*. 2021;14:246–255. doi: [10.1007/s12265-020-10051-2](https://doi.org/10.1007/s12265-020-10051-2)
 73. Abbas ZSB, Latif ML, Dovlatova N, Fox SC, Heptinstall S, Dunn WR, Ralevic V. UDP-sugars activate P2Y14 receptors to mediate vasoconstriction of the porcine coronary artery. *Vasc Pharmacol*. 2018;103-105:36–46. doi: [10.1016/j.vph.2017.12.063](https://doi.org/10.1016/j.vph.2017.12.063)
 74. Sansbury BE, DeMartino AM, Xie Z, Brooks AC, Brainard RE, Watson LJ, DeFilippis AP, Cummins TD, Harbeson MA, Brittain KR, et al. Metabolomic analysis of pressure-overloaded and infarcted mouse hearts. *Circ Heart Fail*. 2014;7:634–642. doi: [10.1161/CIRCHEARTFA.114.001151](https://doi.org/10.1161/CIRCHEARTFA.114.001151)
 75. Wang TJ, Ngo D, Psychogios N, DeJarnat A, Larson MG, Vasani RS, Ghorbani A, O'Sullivan J, Cheng S, Rhee EP, et al. 2-Aminoadipic acid is a biomarker for diabetes risk. *J Clin Invest*. 2013;123:4309–4317. doi: [10.1172/JCI64801](https://doi.org/10.1172/JCI64801)
 76. Saremi A, Howell S, Schwenke DC, Bahn G, Beisswenger PJ, Reaven PD, Investigators V. Advanced glycation end products, oxidation products, and the extent of atherosclerosis during the VA diabetes trial and follow-up study. *Diabetes Care*. 2017;40:591–598. doi: [10.2337/dc16-1875](https://doi.org/10.2337/dc16-1875)
 77. Hannoush H, Introne WJ, Chen MY, Lee SJ, O'Brien K, Suwannarat P, Kayser MA, Gahl WA, Sachdev V. Aortic stenosis and vascular calcifications in alkaptonuria. *Mol Genet Metab*. 2012;105:198–202. doi: [10.1016/j.ymgme.2011.10.017](https://doi.org/10.1016/j.ymgme.2011.10.017)
 78. Russ M, Jauk S, Wintersteiger R, Andra M, Brcic I, Ortner A. Investigation of antioxidative effects of a cardioprotective solution in heart tissue. *Mol Cell Biochem*. 2019;461:73–80. doi: [10.1007/s11010-019-03591-y](https://doi.org/10.1007/s11010-019-03591-y)
 79. Uddin GM, Zhang L, Shah S, Fukushima A, Wagg CS, Gopal K, Al Batran R, Pherwani S, Ho KL, Boisvenue J, et al. Impaired branched chain amino acid oxidation contributes to cardiac insulin resistance in heart failure. *Cardiovasc Diabetol*. 2019;18:86. doi: [10.1186/s12933-019-0892-3](https://doi.org/10.1186/s12933-019-0892-3)
 80. Bullo M, Papandreou C, Garcia-Gavilan J, Ruiz-Canela M, Li J, Guasch-Ferre M, Toledo E, Clish C, Corella D, Estruch R, et al. Tricarboxylic acid cycle related-metabolites and risk of atrial fibrillation and heart failure. *Metabolism*. 2021;125:154915. doi: [10.1016/j.metabol.2021.154915](https://doi.org/10.1016/j.metabol.2021.154915)
 81. Tang X, Liu J, Dong W, Li P, Li L, Lin C, Zheng Y, Hou J, Li D. The cardioprotective effects of citric acid and L-malic acid on myocardial ischemia/reperfusion injury. *Evid Based Complement Alternat Med*. 2013;2013:820695. doi: [10.1155/2013/820695](https://doi.org/10.1155/2013/820695)

SUPPLEMENTAL MATERIAL

Supplemental Methods

Data S1. List of Enrolling Centers

Barnes-Jewish Hospital, St. Louis, MO

Cleveland Clinic Foundation, Cleveland, OH

Dartmouth-Hitchcock Medical Center, Lebanon, NH

Intermountain Heart Institute, Murray, UT

Massachusetts General Hospital, Boston, MA

Morristown Medical Center, Morristown, NJ

Stanford Medical Center, Palo Alto, CA

University of Texas Southwestern Medical Center, Dallas, TX

University of Utah Hospital, Salt Lake City, UT

Vanderbilt University Medical Center, Nashville, TN

Data S2.

Metabolite profiling using liquid chromatography-mass spectrometry.

Methods for metabolite quantification were reproduced directly from other work to enhance rigor and reproducibility

(<https://www.patentsencyclopedia.com/app/20080261317>; Date Accessed 1 May 2023)⁵⁰. Venous blood was processed within 30 minutes of collection and stored at -80°C.

Amino acids and amines, sugars and ribonucleotides, and organic acids were separated by liquid chromatography. Columns were connected in parallel with an automated switching valve on a robotic sample loader (Leap Technologies). A triple-quadrupole mass spectrometer (API4000, Applied Biosystem/ Sciex) operated in automated switching polarity mode with a turbo ion spray LC-MS interface under selected reaction monitoring conditions. Either positive or negative ions were selected for targeted tandem mass spectrometry (MS/MS) analysis using selective reaction conditions. Quantification was performed by integrating peak areas for parent/daughter ion pairs. Metabolite concentrations ≤ 0 were treated as missing (0.001%). We excluded metabolites with $\geq 10\%$ missingness (4/225), and imputed missing values for any metabolite with $< 10\%$ missingness by half of the minimum value detected for that metabolite (0.1% of metabolite measurements). Two subjects had metabolite quantification duplicated, we used the mean concentration for these subjects in analysis.

Principal components analysis to summarize echocardiographic data into 3 axes

of cardiac structure/function. Given the relatedness among the different echocardiographic measures (**Figure S2**), we elected to summarize echocardiographic measures into different, related “axes” of remodeling/function using principal components analysis (PCA; with echocardiographic measures log-transformed to reduce skewness and standardized to unit variance). In this unsupervised PCA approach, the relations among phenotypes were used to collapse the 12 echocardiographic measures into 3 composite axes in an unbiased manner (selected based on examination of variance explained on a scree plot). Broadly, the contribution of each of the 12 echocardiographic measures to each of 3 PCs was quantitated as the loading for the PC (**Figure 2A**). Study participants had a score for each of the 3 PCs that summarized the aspect of their cardiac structure/function captured by that PC. Varimax post-rotation for 3 PCs was used to improve interpretability of loadings across PCs. Scores for each participant represented composite axes of cardiac structure/function and used as the dependent variable in subsequent LASSO models, thereby capturing a broad array of related echocardiographic measures to supervise selection of metabolites most closely related to those axes. While we acknowledge there are many different additional approaches that could be used here (e.g., pre-selecting phenotypes and using those for penalized regression, clustering methods, etc.), we felt that this approach would preserve power to develop optimal models for discovery while limiting type 1 error (due to multiple biomarker testing) that may reduce reproducibility.

Recalibration of LASSO models for use in the single center validation cohort. Given that the metabolites quantified in the single-center validation cohort did not completely match the metabolites measured in our multi-center cohort, we used the metabolites that overlapped between the single-center validation and the multi-center cohort (78 metabolites) to refit models in the multi-center derivation cohort. In these models, the original metabolite score (based on

the “full” LASSO regressions across all metabolites in derivation) was the dependent variable, and the overlapping metabolites were the independent variables. We used a LASSO model for this recalibration effort to mitigate overfitting, generating coefficients that could be applied to overlapping metabolites in the single-center validation cohort to generate the 3 metabolite scores.

Table S1: Metabolite Correlation with Echocardiographic Parameters from LASSO

Metabolite	HMDB	LASSO Coefficient			Biological Significance
		PC1	PC2	PC3	
Phosphocreatine	HMDB0001511	-0.084	-	-	Derivative of amino acid creatine. Plays important role in ATP generation for cardiac contraction ^{51,52} .
Nicotinamide N-Oxide	HMDB0002730	-0.087	-	-0.014	Antagonizes CXCR2 which recruits granulocytes ⁵³ .
N-Docosanoyl Taurine	NA	0.072	-	-	Taurine-conjugated fatty acid.
Adenine	HMDB0000034	0.068	-	-	Nucleic acid.
Serine	HMDB0000187	0.053	0.019	-	Amino acid.
N-Palmitoyltaurine	HMDB0240594	0.059	-	-	Derivative of hexadecenoic acid (fatty acid).
Tryptophan	HMDB0000929	0.045	-	-	Amino acid.
N-Acetyl-L-Phenylalanine	HMDB0000512	0.052	-	-	Derivative of amino acid phenylalanine.
Aconitic acid	HMDB0000072	-0.044	-	-	TCA cycle intermediate. Associated with aortic stenosis ⁵⁴ .
Bilirubin	HMDB0000054	0.043	-	-	Derivative of heme. Associated with mortality among subjects undergoing TAVI ⁵⁵ .
C9 acylcarnitine	HMDB0013288	0.045	-	-	Medium chain acylcarnitine.
Oleoyl glycine	HMDB0013631	-0.038	-	-	Long chain fatty acyl glycine.
Creatine	HMDB0000064	-0.039	0.051	0.036	Amino acid with role in myocardial contraction ⁵² .
Phosphocholine	HMDB0001565	-0.038	-	-	Product of choline kinase to dephosphorylate ATP.
2'-deoxycytidine	HMDB0000014	0.045	-	-	Deoxyribonucleoside.
N-Acetyl-L-Glutamic acid	HMDB0001138	-0.032	-	-	Derivative of L-glutamic acid.
Aspartic acid	HMDB0000191	0.031	0.074	-	Amino acid.
N-Acetyl-L-Ornithine	HMDB0003357	-0.020	-	-	Derivative of amino acids arginine and proline.
2-Hydroxybutyric acid	HMDB0000008	-0.024	-	-	Organic acid from amino acid metabolism (threonine and methionine). A marker of insulin resistance ⁵⁶ .
Sarcosine	HMDB0000271	-0.020	-	-	Derivative of amino acid glycine.
C26 acylcarnitine	HMDB0002356	0.020	-	-	Long chain acylcarnitine. An intermediate of fatty acid metabolism, associated with LV remodeling in AS ¹² .
Saccharopine	HMDB0000279	-0.025	-	-	Derivative of amino acid lysine.
Glycocholic acid	HMDB0000138	-0.023	-	-	Bile acid conjugate of glycine and choline.
Kynurenine	HMDB0000684	0.033	-	-	Metabolite of tryptophan (amino acid) that has been

					shown to suppress immune response ⁵⁷ . Associated with survival among patients with heart failure ³¹ .
Lactic acid	HMDB0000190	-0.030	-	-	Organic acid derivative of glucose metabolism. May play a in modulating hypertrophy and heart failure ⁵⁸ .
Choline	HMDB0000097	0.013	-	-	Associated with cardiovascular disease ^{36,59} . Associated with LV remodeling in AS ¹² .
DDHAP / Glyceraldehyde 3-phosphate	HMDB0001112	-0.019	-0.037	-	Derivative of glucose metabolism.
DiHOME	HMDB0004705	-0.018	-	-	Linoleic acid metabolite. Increases fatty acid uptake in skeletal muscle ⁶⁰ .
Dihomo-γ-Linolenoyl Ethanolamide	HMDB0013625	0.020	0.008	-	Endocannabinoid.
Uracil	HMDB0000300	-0.008	-	-	Nucleobase of RNA. May play a role in cardiac hypertrophy ³⁰ .
Glucose/Fructose/Galactose	HMDB0000122 (glucose)	-0.022	-	-	Monosaccharides.
Cystine	HMDB0000192	-0.010	-	-	Amino acid. Associated with diastolic dysfunction ⁶¹ .
Glycochenodeoxycholic acid	HMDB0304944	-0.003	-	-	Bile salt.
N-carbomoyl-beta-alanine	HMDB0000026	0.009	-0.028	-	Derivative of amino acid uracil.
C18.2 carnitine	HMDB0006469	0.017	-	-	An intermediate of fatty acid metabolism, associated with LV remodeling in AS ¹² . Related to coronary artery disease ³³ .
Histamine	HMDB0000870	-0.001	-	-	Imidazole. May play a role in the development of heart failure and cardiac fibrosis after MI ^{62,63} .
Cyclic AMP	HMDB0000058	-0.007	-	-	Derivative of adenosine triphosphate used in intracellular signaling for a variety of pathways.
Anserine	HMDB0000194	-0.004	-	-	A dipeptide derivative of carnosine.
Cytidine	HMDB0000089	0.003	-	-	Nucleoside component of RNA.
α-Ketoglutaric acid	HMDB0000208	-	-0.100	-	TCA cycle intermediate. In a murine model, supplementation lessened pressure-overload cardiac hypertrophy and preserved systolic function ³⁵ .
Beta-alanine	HMDB0000056	-	-0.086	-	Amino acid. Supplementation shown to improve response to strength training in humans ⁶⁴ and functional capacity

					in a murine model of heart failure ⁶⁵ .
Glutamate	HMDB0000148	-	-0.059	-	Amino acid and a common neurotransmitter. Used in some formulations of cardioplegia due to possible improvements in outcomes ⁶⁶ . Shown to reduce oxidative injury in a murine model of myocardial infarction ⁶⁷ . Associated with increased risk of stroke ⁶⁸ .
Uridine	HMDB0000296	-	0.058	-	Nucleic acid. Supplementation reduced ischemic reperfusion injury in a murine model ⁶⁹ . Associated with incident heart failure in the Jackson Heart Study ³⁶ .
Uridine (anode)	HMDB0000296	-	0.018	-	
Arginine	HMDB0000517	-	0.052	-	Amino acid and precursor of nitric oxide in the vascular endothelium. Supplementation in subjects with ischemic heart failure had improved function and dimensions ⁷⁰ .
Glycine	HMDB0000123	-	0.057	-	Amino acid. Elevated in subjects with severe heart failure ⁷¹ . Glycine metabolism is different after exercise in subjects with hypertrophic cardiomyopathy ⁷² .
UDP-glucose / UDP-galactose	HMDB0000286 (glucose)	-	-0.050	-	Nucleotide sugar. Involved in carbohydrate metabolism. Implicated as a coronary vasoconstrictor ⁷³ .
Spermidine	HMDB0001257	-	-0.046	-	Polyamine. Elevated in murine models of pressure overload and infarct hearts ⁷⁴ . May be helpful in prognosticating outcomes in heart failure ²⁸ .
2-aminoadipic acid	HMDB0302754	-	-0.031	-	Product of lysine metabolism. Associated with incident heart failure in the Jackson Heart Study ³⁶ and development of T2DM ⁷⁵ and atherosclerosis ⁷⁶ .
N-oleoyl dopamine	HMDB0255218	-	0.020	-	Fatty amide. Protective against ischemia-reperfusion injury ³⁴ .
Tyrosine	HMDB0000158	-	-0.023	-	Amino acid. A disorder of tyrosine catabolism, alkaptonuria, is associated with aortic stenosis ⁷⁷ .
N-Carbamoyl-BAIBA	NA	-	-	0.102	Product of thymine catabolism
S-adenosyl-L-homocysteine	HMDB0000939	-	-	0.076	Sole metabolic precursor to homocysteine and a derivative of amino acids methionine and

					cysteine. Associated with coronary heart disease ³² .
20-Hydroxy N-Arachidonoyl-Taurine	NA	-	-	0.012	Fatty acid amide of amino acid taurine.
Histidine	HMDB0000177	-	-	-0.069	Amino acid. Improved functional capacity in a murine model of heart failure ⁶⁵ .
N-acetyl-L-methionine	HMDB0011745	-	-	0.055	Derivative of amino acid methionine. May be helpful in reducing ischemia-reperfusion injury ⁷⁸
Valine	HMDB0000883	-	-	-0.044	Branched chain amino acid. Defective metabolism may be implicated in heart failure pathogenesis ²¹ and cardiac insulin resistance ⁷⁹ .
Oxaloacetic acid	HMDB0000223	-	-	0.028	Organic acid involved in numerous metabolic pathways.
Leucine	HMDB0000687	-	-	-0.006	Branched chain amino acid. Defective metabolism may be implicated in heart failure pathogenesis ²¹ and cardiac insulin resistance ⁷⁹ .
Malic acid	HMDB0000156	-	-	0.004	TCA cycle intermediate. Associated with atrial fibrillation and heart failure ⁸⁰ . Reduced ischemia reperfusion injury in mice ⁸¹ .

ATP = adenosine triphosphate; CXCR2 = chemokine (CXC motif) receptor 2; TCA = tricarboxylic acid; TAVI = transcatheter aortic valve implantation; LV = left ventricular; AS = aortic stenosis; RNA = Ribonucleic acid; MI = myocardial infarction; T2DM = type 2 diabetes mellitus.

Table S2: Spearman correlation between phenotype scores, metabolite scores, select echocardiographic variables (exemplary of each PC-based phenotype category), and multi-morbidity measures from the multi-center derivation cohort. N represents the number of observations on which the correlation is based (not all individuals had every measure). The P-value reported is the nominal P-value for the correlation, **Figure 4** in the manuscript uses an asterisk to indicate which P-values passed a false discovery rate of 5% (Benjamini-Hochberg). Of note, phenotype scores were not calculated in the multi-center validation cohort due to incomplete echocardiographic data (see **Table 1**). eGFR = estimate glomerular filtration rate, FEV1 = Forced expiratory volume in the first second; PC = principal component; LVEDVI = left ventricular end-diastolic volume index; LVEF = left ventricular ejection fraction.

Correlation coefficient									
	PC1	Metabolite -PC1	LVEDVI	PC2	Metabolite -PC2	LVEF	PC3	Metabolite -PC3	Mean E/e'
Age (N=519)	-0.002	0.022	-0.107	0.045	0.108	0.009	0.141	0.067	0.036
Kansas City Cardiomyopathy Questionnaire summary score (N=487)	-0.033	-0.044	-0.038	0.167	0.236	0.130	-0.222	-0.286	-0.169
Average grip strength (N=475)	0.141	0.116	0.207	-0.118	-0.253	-0.190	-0.164	-0.138	-0.195
Average gait speed (N=458)	0.116	-0.036	0.127	0.005	0.141	-0.031	-0.182	-0.281	-0.173
Mini-Cog total score (N=484)	-0.024	0.013	0.023	-0.037	-0.006	-0.031	-0.102	-0.051	-0.030
FEV1, % Predicted (N=410)	-0.103	-0.166	-0.121	0.204	0.256	0.218	-0.085	-0.157	-0.082
Hemoglobin (N=516)	-0.059	-0.147	-0.083	-0.142	-0.088	-0.033	-0.216	-0.359	-0.242
Platelets (N=515)	-0.020	-0.097	-0.043	-0.035	0.030	-0.014	-0.020	0.016	0.064
Uric Acid (N=504)	0.058	0.170	0.096	-0.054	-0.199	-0.096	0.129	0.299	0.045
eGFR (N=517)	-0.019	-0.158	-0.033	-0.041	0.042	0.038	-0.211	-0.509	-0.203

P-value of correlation									
Age	9.69E-01	6.10E-01	1.49E-02	3.06E-01	1.37E-02	8.39E-01	1.26E-03	1.25E-01	4.15E-01
Kansas City Cardiomyopathy Questionnaire summary score	4.63E-01	3.36E-01	4.01E-01	2.16E-04	1.45E-07	3.94E-03	7.58E-07	1.22E-10	1.80E-04
Average grip strength	2.04E-03	1.11E-02	5.49E-06	1.04E-02	2.35E-08	3.02E-05	3.18E-04	2.67E-03	1.83E-05
Average gait speed	1.30E-02	4.37E-01	6.37E-03	9.15E-01	2.48E-03	5.04E-01	8.95E-05	8.67E-10	1.95E-04
Mini-Cog total score	5.92E-01	7.72E-01	6.09E-01	4.18E-01	8.94E-01	5.02E-01	2.44E-02	2.62E-01	5.05E-01
FEV1, % Predicted	3.66E-02	7.29E-04	1.39E-02	3.29E-05	1.52E-07	8.81E-06	8.67E-02	1.45E-03	9.75E-02
Hemoglobin	1.83E-01	7.95E-04	5.84E-02	1.20E-03	4.66E-02	4.53E-01	7.60E-07	<2.20E-16	2.56E-08
Platelets	6.43E-01	2.76E-02	3.31E-01	4.24E-01	4.90E-01	7.53E-01	6.45E-01	7.10E-01	1.45E-01
Uric Acid	1.97E-01	1.26E-04	3.07E-02	2.25E-01	6.94E-06	3.18E-02	3.82E-03	7.08E-12	3.17E-01
eGFR	6.61E-01	3.11E-04	4.52E-01	3.51E-01	3.37E-01	3.90E-01	1.31E-06	<2.20E-16	3.13E-06

Table S3: Spearman correlation between phenotype scores, metabolite scores, select echocardiographic variables (exemplary of each PC-based phenotype category), and multi-morbidity measures in the multi-center validation cohort. N represents the number of observations on which the correlation is based (not all individuals had every measure). The P-value reported is the nominal P-value for the correlation, **Figure 4** in the manuscript uses an asterisk to indicate which P-values passed a false discovery rate of 5% (Benjamini-Hochberg). Of note, phenotype scores were not calculated in the multi-center validation cohort due to incomplete echocardiographic data (see **Table 1**). eGFR = estimate glomerular filtration rate, FEV1 = Forced expiratory volume in the first second.

Correlation coefficient			
	Metabolite-PC1	Metabolite-PC2	Metabolite-PC3
Age (N=286)	0.150	0.100	0.093
Left ventricular ejection fraction (N=260)	-0.177	0.158	-0.273
Left ventricular end diastolic volume index (N=120)	0.139	-0.173	0.237
Mean E/e' (N=79)	0.170	0.005	0.359
Average gait speed (N=226)	-0.065	0.151	-0.316
Average grip strength (N=251)	0.033	-0.142	-0.114
Kansas City Cardiomyopathy Questionnaire summary score (N=267)	-0.017	0.170	-0.200
FEV1, % predicted (N=192)	0.023	0.189	-0.225
Mini-Cog total score (N=265)	0.066	0.062	0.010

Hemoglobin (N=284)	-0.168	-0.114	-0.298
Platelets (N=284)	-0.080	0.018	0.033
Uric acid (N=276)	0.192	-0.202	0.300
eGFR (N=283)	-0.202	0.146	-0.523
P-value of correlation			
Age	1.11E-02	9.18E-02	1.18E-01
Left ventricular ejection fraction	4.17E-03	1.08E-02	8.13E-06
Left ventricular end diastolic volume index	1.31E-01	5.94E-02	9.11E-03
Mean E/e'	1.34E-01	9.66E-01	1.17E-03
Average gait speed	3.31E-01	2.30E-02	1.28E-06
Average grip strength	6.03E-01	2.48E-02	7.15E-02
Kansas City Cardiomyopathy Questionnaire summary score	7.88E-01	5.45E-03	1.05E-03
FEV1, % predicted	7.56E-01	8.69E-03	1.74E-03
Mini-Cog total score	2.81E-01	3.15E-01	8.75E-01
Hemoglobin	4.46E-03	5.56E-02	3.04E-07
Platelets	1.78E-01	7.58E-01	5.81E-01
Uric acid	1.34E-03	7.29E-04	3.87E-07
eGFR	6.42E-04	1.43E-02	<2.20E-16

Table S4: Cox models for all-cause mortality. Hazard ratios represent risk for a 1 standard deviation increase. “Adjusted” models in the derivation and multi-center validation cohorts were adjusted for age, sex, body mass index, history of diabetes mellitus, history of coronary artery disease, history of atrial fibrillation or flutter, estimated glomerular filtration rate, high sensitivity troponin, and N-terminal pro hormone B-type natriuretic peptide. “Adjusted” models in the single-center validation cohort were adjusted for age, sex, body mass index, history of diabetes mellitus, history of coronary artery disease, history of atrial fibrillation or flutter, estimated glomerular filtration rate, and B-type natriuretic peptide. “Sensitivity” models include additional adjustments for mean aortic valve gradient and left ventricular ejection fraction. PC = principal component.

		Metabolite-based				Phenotype-based			
		N	Deaths	Hazard Ratio (95% CI)	P-value	N	Deaths	Hazard Ratio (95% CI)	P-value
Derivation	Unadjusted								
	PC1	516	205	1.27 (1.11-1.45)	0.001	516	205	1.01 (0.88 – 1.16)	0.88
	PC2	516	205	0.84 (0.73-0.97)	0.02	516	205	0.84 (0.73 – 0.96)	0.01
	PC3	516	205	1.75 (1.55-1.99)	<0.001	516	205	1.40 (1.22 – 1.62)	<0.001
	Adjusted								
	PC1	494	198	0.98 (0.84-1.15)	0.81	494	198	0.83 (0.70 – 0.98)	0.02
	PC2	494	198	0.94 (0.80-1.10)	0.42	494	198	0.90 (0.78 – 1.05)	0.18
	PC3	494	198	1.54 (1.25-1.90)	<0.001	494	198	1.09 (0.91 – 1.29)	0.34
	Sensitivity								
	PC1	494	198	1.01 (0.86-1.19)	0.87			-	
PC2	494	198	0.95 (0.81-1.12)	0.53			-		
PC3	494	198	1.55 (1.26-1.92)	<0.001			-		
Multi-center Validation	Unadjusted								
	PC1	282	121	1.10 (0.92-1.33)	0.28			-	
	PC2	282	121	0.77 (0.64-0.93)	0.008			-	
	PC3	282	121	1.58 (1.34-1.87)	<0.001			-	
	Adjusted								
	PC1	274	116	0.94 (0.76-1.16)	0.58			-	
	PC2	274	116	0.90 (0.73-1.11)	0.32			-	
PC3	274	116	1.37 (1.05-1.78)	0.02			-		
Single-center Validation	Unadjusted								
	PC1	257	93	1.17 (0.94-1.44)	0.16			-	
	PC2	257	93	0.93 (0.76-1.13)	0.44			-	
	PC3	257	93	1.37 (1.13-1.67)	0.001			-	
	Adjusted								
	PC1	251	91	1.11 (0.86-1.43)	0.43			-	
	PC2	251	91	0.88 (0.72-1.09)	0.25			-	
PC3	251	91	1.43 (1.06-1.92)	0.02			-		

Table S5: Results of the "recalibrated" LASSO model using metabolites common to both internal derivation and external validation cohorts. LASSO = least absolute shrinkage and selection operator; PC = principal component.

metabolite	LASSO Coefficient		
	PC1	PC2	PC3
glycine	0.01494987	0.139102307	0.030239001
alanine	-0.251512522	-0.113791394	0.024166223
serine	0.143051865	0.106803934	-0.041300673
threonine	0.050589769	0.033504175	0.040275094
methionine	-	-0.05081661	-
aspartate	0.015995975	-	0.080618582
glutamate	-	-0.16867989	-0.033268046
asparagine	-	0.042200172	-0.086920091
glutamine	-0.005139735	0.022095756	-
histidine	-0.069711788	0.074003134	-0.332893973
arginine	-0.030562809	0.212603096	-0.016608614
lysine	-	0.041159659	-0.001146626
valine	-0.101041903	0.000266757	-0.167696977
leucine	-	0.045187493	-0.110701583
phenylalanine	0.084663329	-	0.048414897
tyrosine	-	-0.114599243	0.002947603
tryptophan	0.101032064	-0.013813357	-0.029229131
proline	-0.053258912	-0.012065449	-0.01105175
cis.trans.hydroxyproline	-	-	-
ornithine	-	-0.068995475	-
citrulline	0.016689991	0.029839466	0.012033922
taurine	0.025119423	-	-
5.hydroxytryptophan	-	-	-0.017393582
5.HIAA	-	-0.006672996	0.042201013
cystamine	-0.062069023	0.013839851	-0.001509095
cysteamine	0.030232505	-0.000299186	-0.007223417
GABA	-	-0.01236756	-0.013089138
dimethylglycine	0.017769162	-	-
homocysteine	-	-0.008340423	-0.001346062
ADMA.SDMA	0.010550956	0.052037309	0.166046764
NMMA	-	-	-
allantoin	-	0.005085548	0.115265873

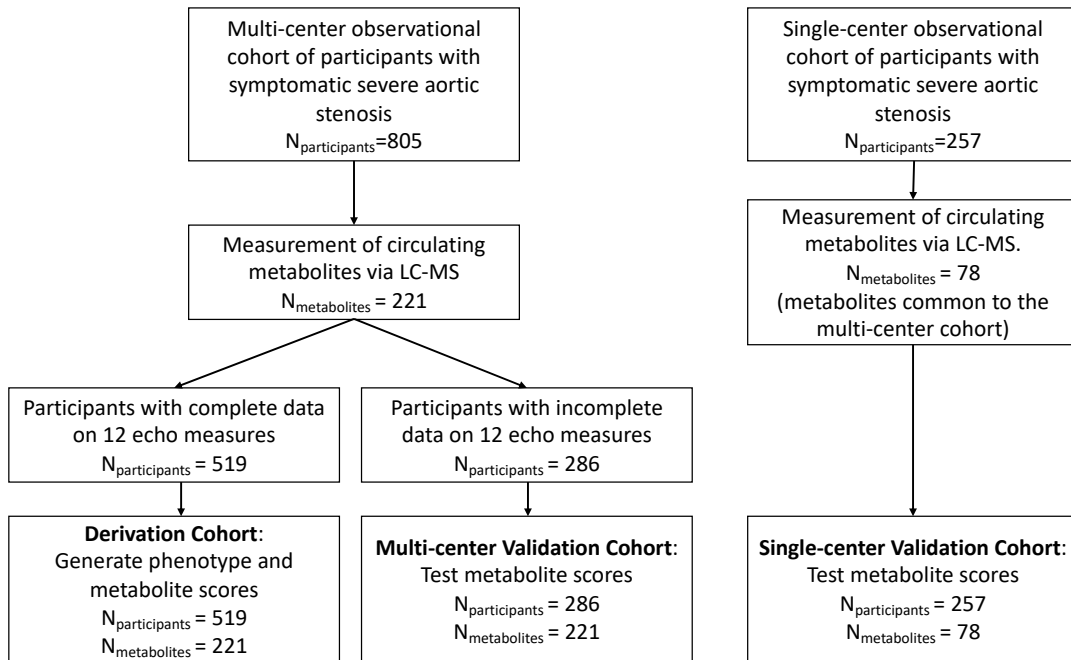
aminoisobutyric.acid	0.008684823	0.020307994	-
carnitine	-	-0.015765839	-0.056224754
1.methylhistamine	-	-0.027932122	0.023886073
5..adenosylhomocysteine	-	-	0.01108117
3.hydroxyanthranilic.acid	-	-	-0.05508892
N.carbomoyl.beta.alanine	0.113717016	-0.18009016	0.281661982
niacinamide	-0.157019631	0.006085806	-
betaine	0.016686918	0.011834496	-0.011957004
choline	0.009601636	-	0.006595445
phosphocholine	-0.1747666	-	-0.021421928
alpha.glycerophosphocholine	-	0.037644223	0.005717554
spermidine	-0.04104223	-0.191238112	-0.095427795
creatine	-0.158601676	0.132805505	0.188000128
creatinine	0.086683549	-	0.114546392
adenosine	0.037085836	0.003767399	-0.022240968
cytosine	-	0.010832363	-
xanthosine	0.00130912	-0.063711329	0.024627807
cAMP	-0.060711268	-0.034277629	-0.001141732
isoleucine	-	-0.021463649	0.017886777
xanthine	-0.048163564	0.032269234	-0.038850884
xanthurenate	0.11585772	-0.095660451	-
kynurenine	0.172680721	0.033820158	0.086083182
uridine	-0.012756245	0.24380548	-0.079669817
citicholine	-0.00029907	-0.134291446	-
beta.alanine	-0.089808244	-0.305192791	-
C2.carnitine	-0.073445173	-0.008632177	-
C3.carnitine	-	-	-0.048265682
C3.malonyl.carnitine	-	-0.067866411	-
C4.butyryl.carnitines	0.053656022	0.000160457	0.056067457
C4.methylmalonyl.carnitine	-0.063571497	-0.016661022	0.017603944
C5.valeryl.carnitines	-	-	-
C5.glutaryl.carnitine	0.013413055	-	0.073555365
C6.carnitine	-	-	0.014374416
C7.carnitine	-	-0.038240411	0.005419971
C8.carnitine	-	0.035161499	-0.016166012
C9.carnitine	0.17198752	-	0.02357368
C10.carnitine	-0.03710882	-	-
C12.carnitine	-	-	0.04619551
C14.carnitine	0.075879056	0.038998555	-0.038372988

C16.carnitine	-	-	0.005230519
C18.carnitine	-0.034616529	0.024214834	-0.081105255
C18.1.carnitine	-	-0.090844535	0.06323825
C18.2.carnitine	0.14104691	-	0.043582665
C26.carnitine	0.051564122	0.044507161	-0.024568913
anandamide	-0.046417867	-	-
Cystine	-0.059824958	-0.034687137	-0.025504188

Table S6: Measures of multimorbidity and frailty in the derivation and multi-center validation cohort. Continuous variables are reported as median (25th, 75th percentile); % missing. Categorical variables are reported as n (%); % missing. FEV₁ = Forced expiratory volume in the first second.

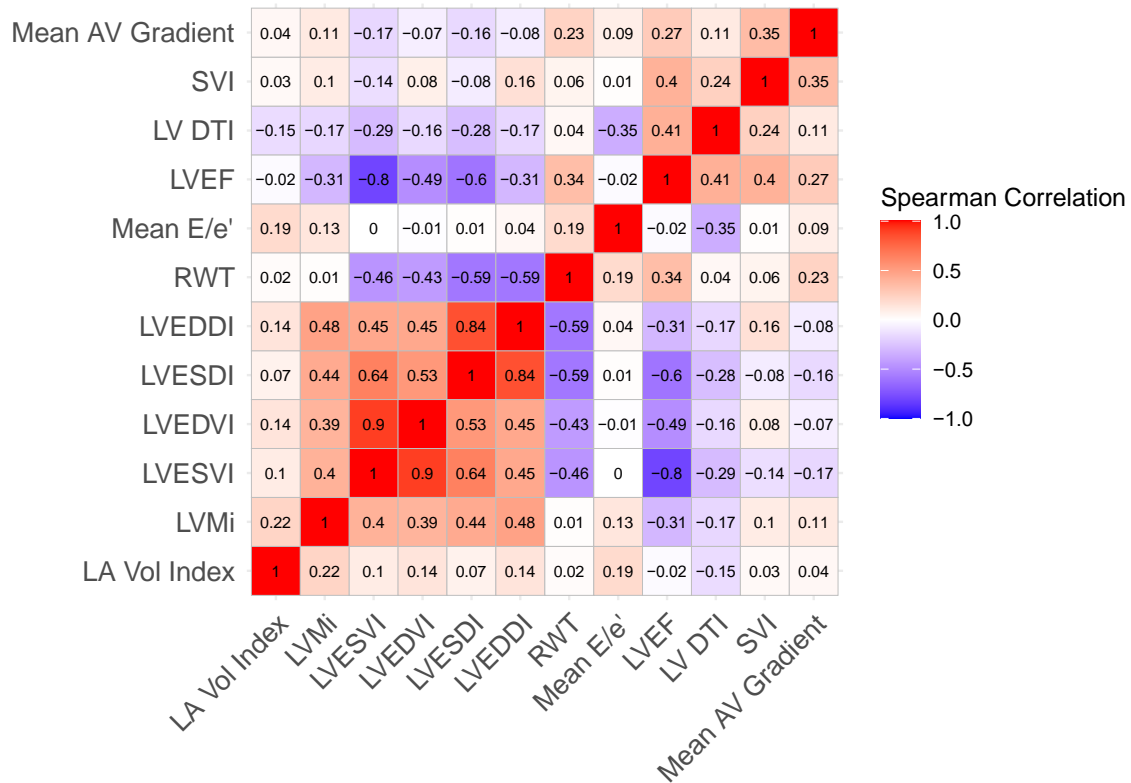
Characteristic	Derivation N = 519	Multi-center Validation N = 286
Kansas City Cardiomyopathy Questionnaire Score	47 (29, 66); 6.2%	46 (30, 64); 6.6%
Gait speed average (m/s)	0.72 (0.55, 0.88); 12%	0.67 (0.51, 0.84); 21%
Grip strength average (kg)	19 (14, 26); 8.5%	19 (13, 27); 12%
Mini-Cog total score	3.00 (2.00, 5.00); 6.7%	3.00 (2.00, 4.00); 7.3%
Percent predicted FEV ₁	82 (67, 102); 21%	75 (60, 90); 33%
Hemoglobin (mg/dL)	12.20 (10.90, 13.30); 0.6%	12.50 (11.20, 13.72); 0.7%
Platelets (per liter)	199 (158, 244); 0.8%	190 (156, 239); 0.7%
Uric acid (mg/dL)	6.30 (5.00, 7.70); 2.9%	6.30 (5.10, 8.00); 3.5%

Figure S1: CONSORT diagram



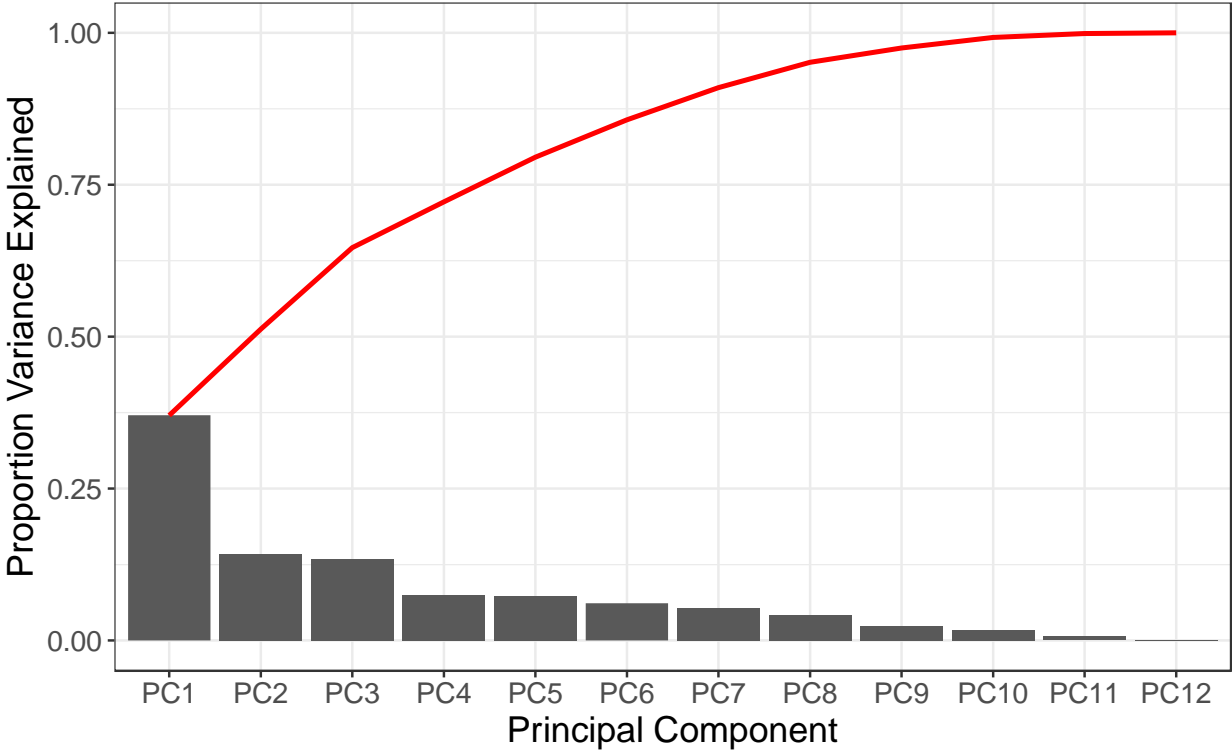
LC-MS = liquid chromatography – mass spectrometry

Figure S2: Correlation of echocardiographic parameters



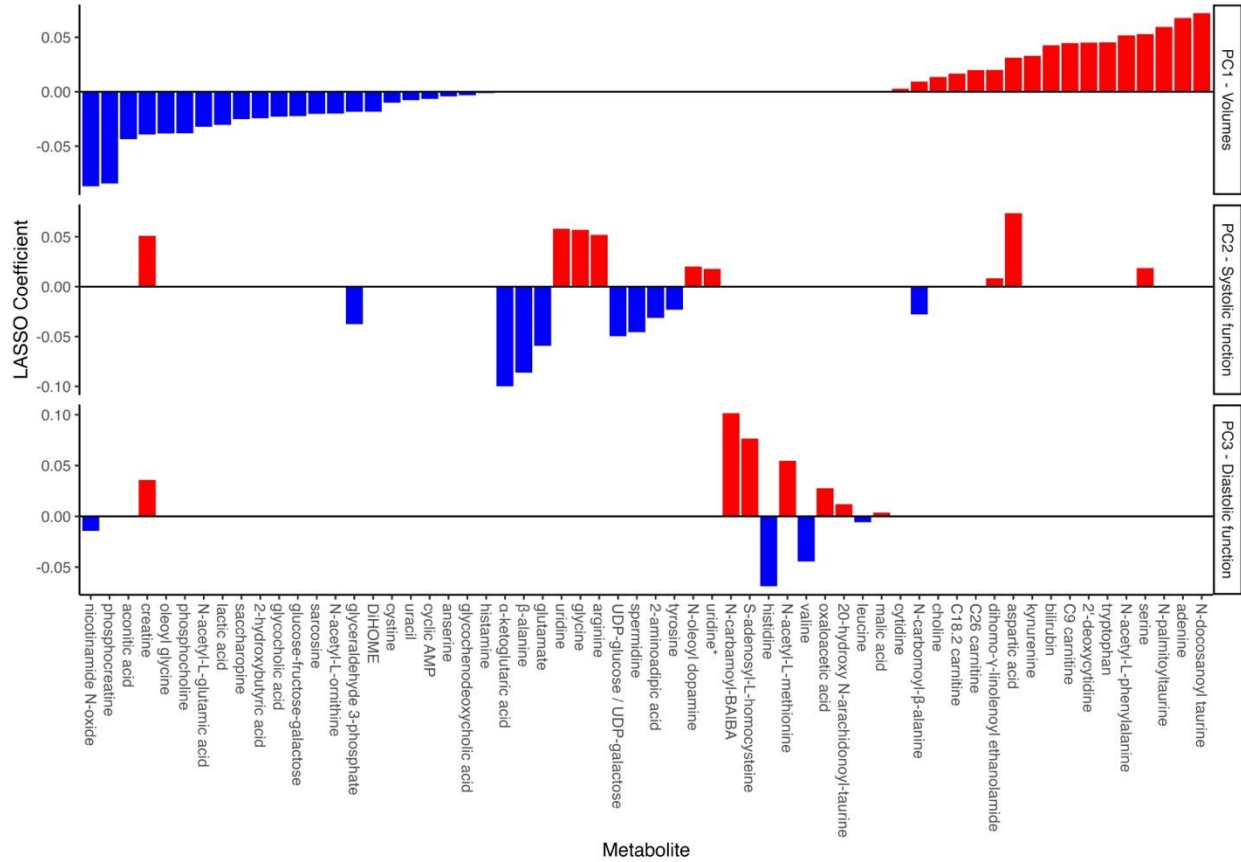
Spearman correlation across 12 echocardiographic parameters used in principal components analysis. LA Vol = left atrium volume index; LVMi = left ventricular mass index; LVESVI = left ventricular end-systolic volume index; LVEDVI = left ventricular end-diastolic volume index; LVESDI = left ventricular end-systolic diameter index; LVEDDI = left ventricular end-diastolic diameter index; RWT = relative wall thickness; LVEF = left ventricular ejection fraction; LV DTI = tissue Doppler S velocity of lateral mitral annulus; SVI = stroke volume index; AV = aortic valve.

Figure S3: Scree plot from principal components analysis



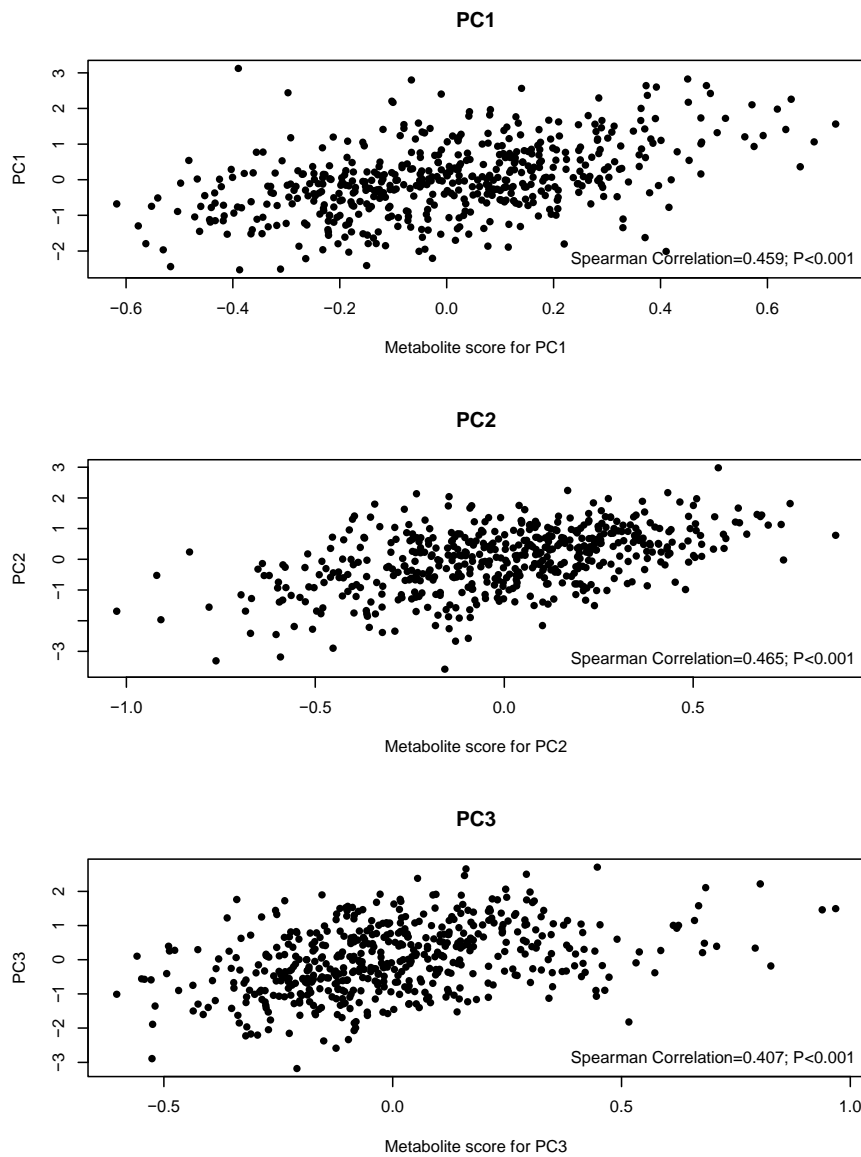
Scree plot demonstrating proportion of variance explained (bars) and cumulative variance explained (red line), suggesting 3 principal components. PC = principal component.

Figure S4: Relationship between circulating metabolites and echocardiographic PCs.



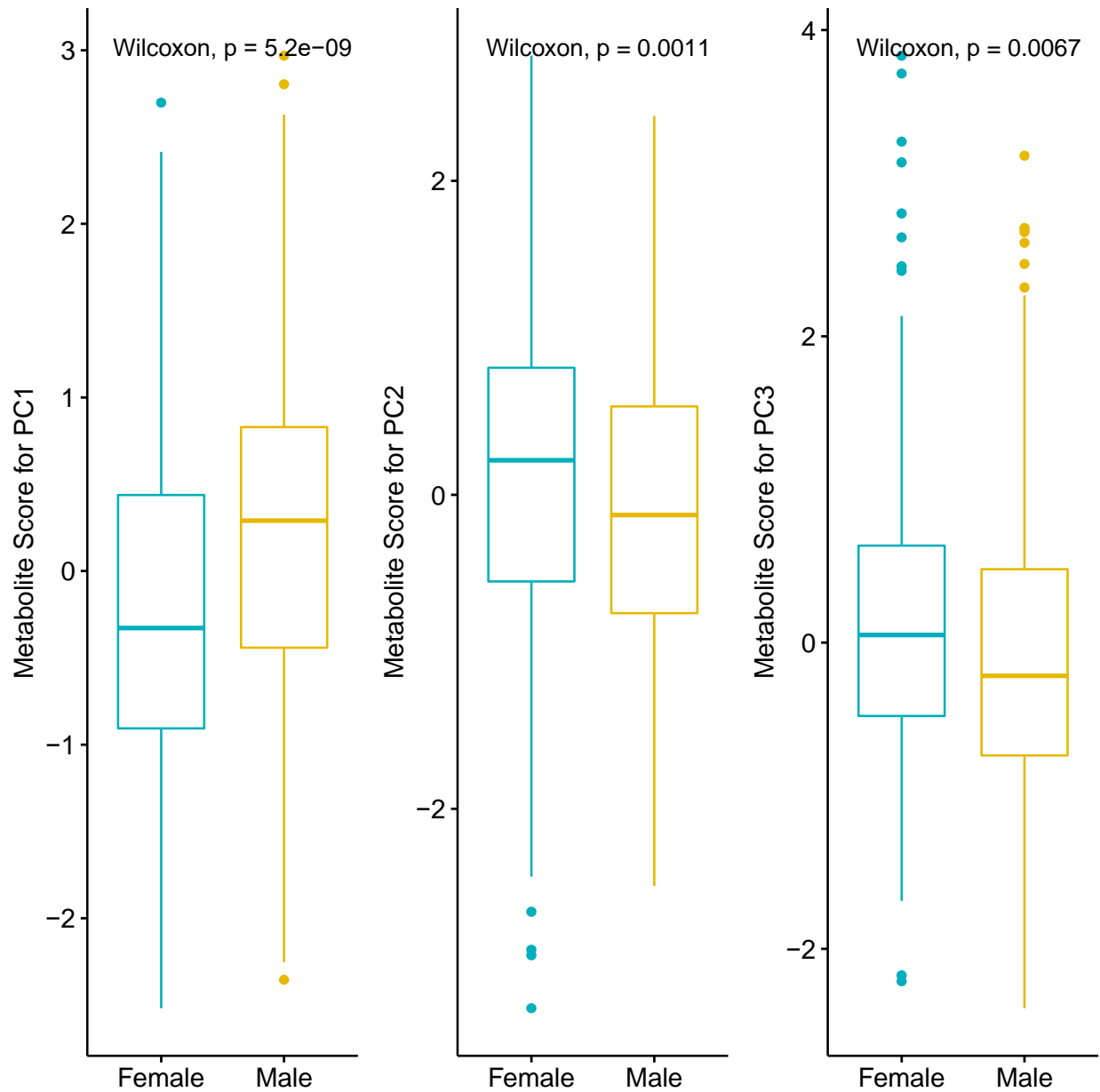
All 60 metabolites selected by LASSO are shown with their corresponding loading with each echocardiographic PC (see **Table S1** for coefficients). LASSO = least absolute shrinkage and selection operator; PC = principal component. *HILIC negative ion mode.

Figure S5: Relation of metabolite scores to parent phenotypes



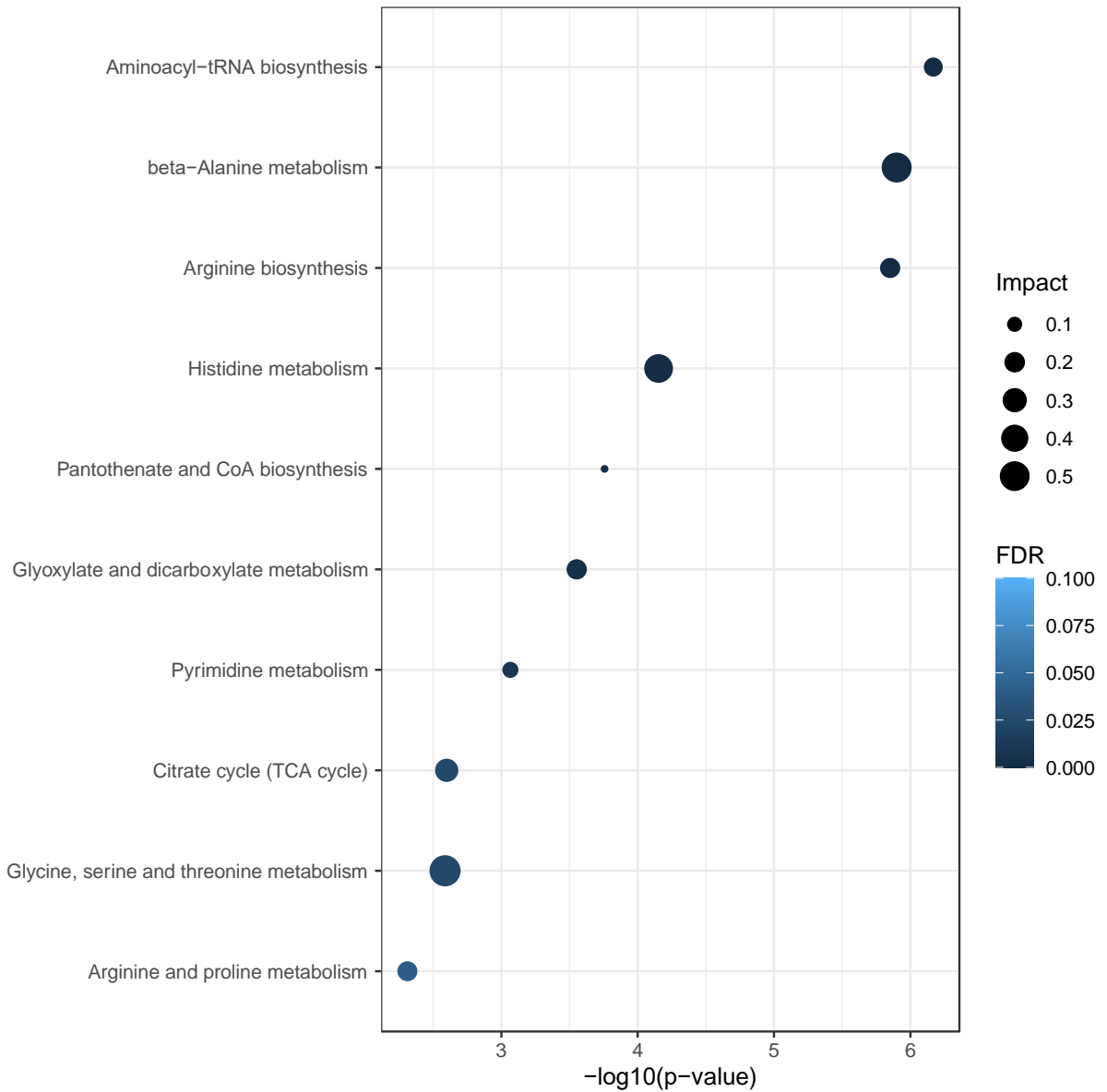
Relation of parent phenotype PC scores with metabolite scores. The associations were moderate in magnitude. Reported R^2 is from model optimization at the optimal lambda. PC = principal component.

Figure S6: Comparison of metabolite scores across sex.



Box-plots for metabolite scores across sex (comparison by Wilcoxon test). While we observed statistically significant differences by sex, there was a broad degree of overlap suggesting no clinically meaningful differences in metabolite score by sex. PC = principal component.

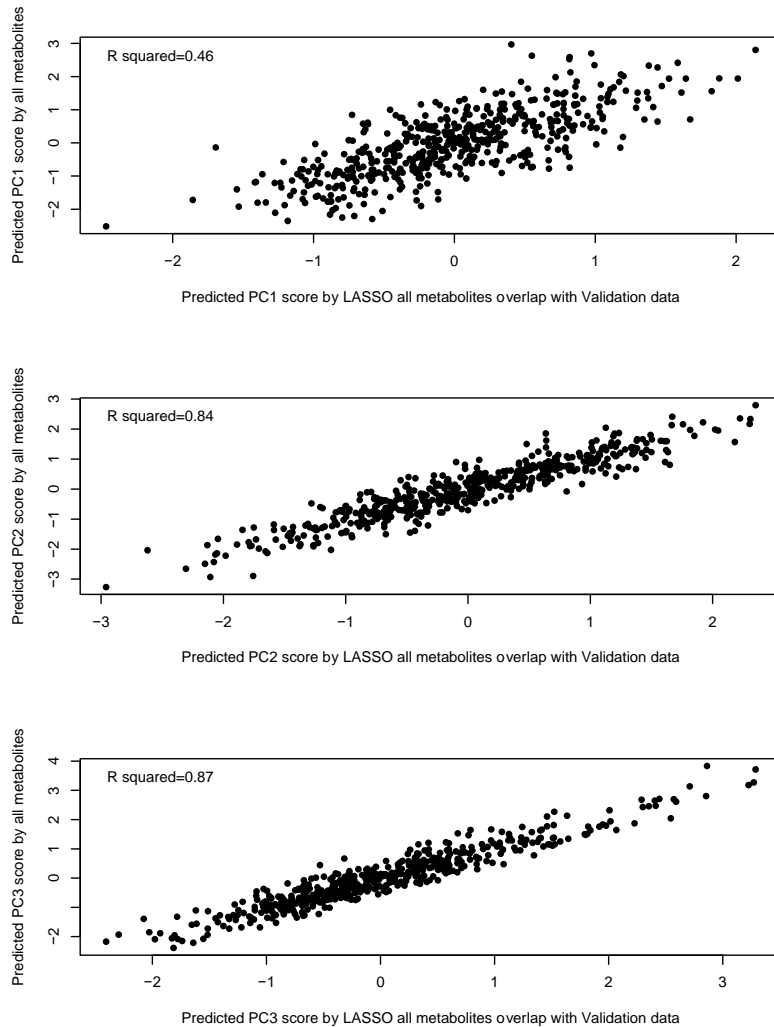
Figure S7: Pathway analysis of metabolite scores



Metabolic pathway analysis of 52 metabolites with Human Metabolome Database (HMDB) identifiers (out of 60 metabolites across all identified metabolite scores).

Pathways with an FDR < 0.05 are shown. FDR = false discovery rate.

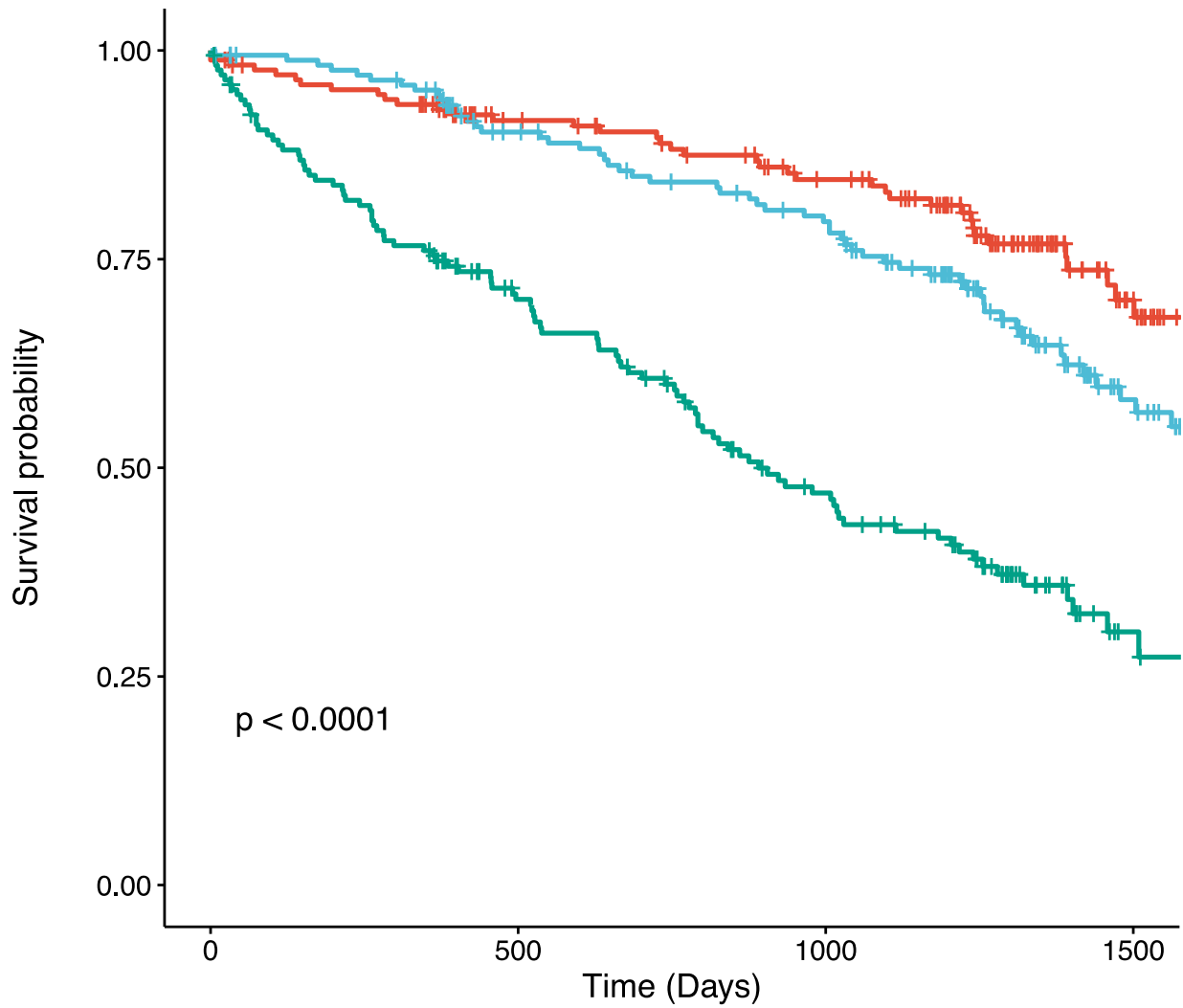
Figure S8: Correlation of recalibrated metabolite scores with original metabolite scores



Recalibration of scores for the single-center validation cohort (as described in **Methods** and **Results**). Axes correspond to the full score (Y axis; based on all metabolites in our derivation sample) versus the recalibrated “reduced” score (X-axis; based on metabolites that overlap between the multi-center derivation cohort and the single-center validation cohort). R^2 is moderate to excellent (up to 87% for PC3). PC = principal component.

Figure S9: Validation of the prognostic utility of the metabolite score for PC3 in separate cohorts.

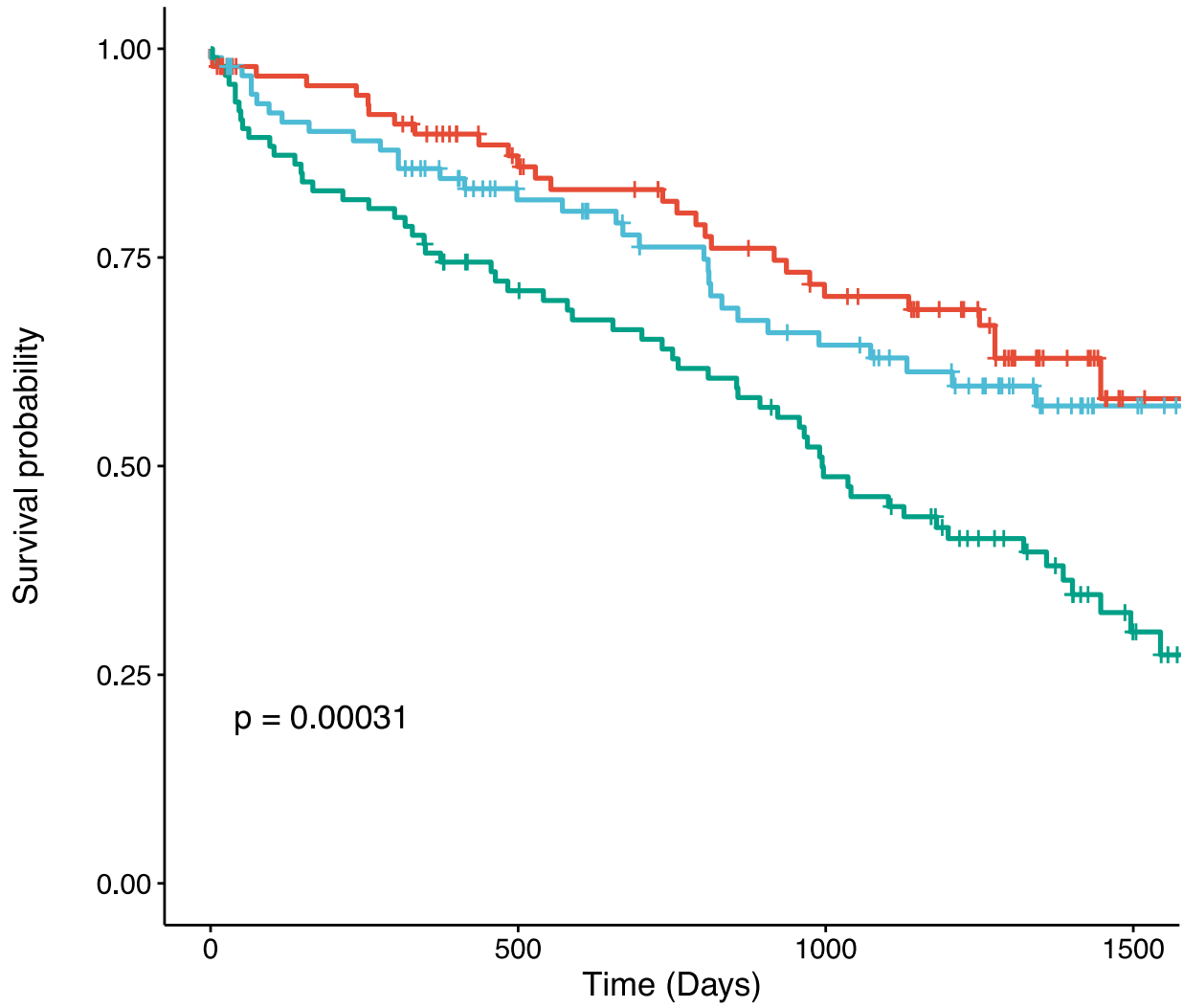
Figure S9A



Metabolite-PC3 Score	Number at risk			
	0	500	1000	1500
Tertile 1	173	136	113	35
Tertile 2	172	138	116	38
Tertile 3	171	104	62	10

Time (Days)

Figure S9B

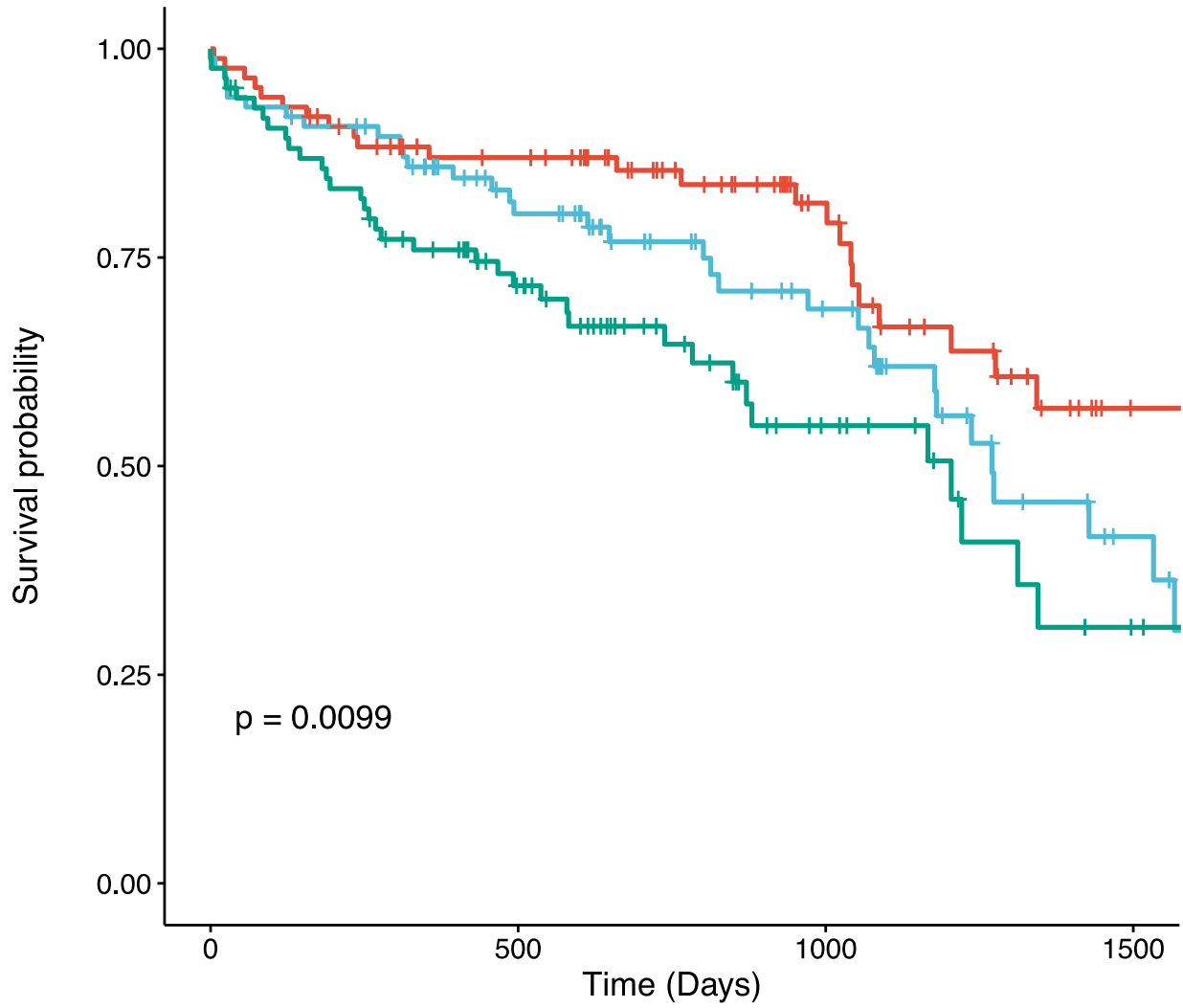


Metabolite-PC3 Score

	Number at risk			
	0	500	1000	1500
Tertile 1	94	65	48	7
Tertile 2	94	61	43	15
Tertile 3	94	62	41	12

Time (Days)

Figure S9C



Metabolite-PC3 Score

	Number at risk			
	0	500	1000	1500
Tertile 1	86	66	34	7
Tertile 2	86	56	31	8
Tertile 3	85	48	17	4

Time (Days)

Kaplan-Meier estimates of survival among the multi-center derivation cohort (A), multi-center validation cohort (B), and single-center validation cohort (C) stratified by tertiles of PC3 metabolite score. For visualization plots are truncated at 1500 days. P-values from logrank tests are reported. PC = principal component.